Measurement of the charge asymmetry in top quark pair production in pp collisions at $\sqrt{s} = 8$ TeV using a template method

CMS Collaboration ; Canelli, F ; Chiochia, V ; Kilminster, B ; Robmann, P ; et al

Abstract: The charge asymmetry in the production of top quark and antiquark pairs is measured in proton-proton collisions at a center-of-mass energy of 8 TeV. The data, corresponding to an integrated luminosity of 19.6 fb^{-1}, were collected by the CMS experiment at the LHC. Events with a single isolated electron or muon, and four or more jets, at least one of which is likely to have originated from hadronization of a bottom quark, are selected. A template technique is used to measure the asymmetry in the distribution of differences in the top quark and antiquark absolute rapidities. The measured asymmetry is A_C^y=[0.33±0.26(stat)±0.33(syst)]%, which is the most precise result to date. The results are compared to calculations based on the standard model and on several beyond-the-standard-model scenarios.

DOI: https://doi.org/10.1103/PhysRevD.93.034014

EUROPEAN ORGANIZATION FOR NUCLEAR RESEARCH (CERN)

CERN-PH-EP/2015-189
2015/08/18

CMS-TOP-13-013

Measurement of the charge asymmetry in top quark pair production in pp collisions at $\sqrt{s} = 8\,\text{TeV}$ using a template method

The CMS Collaboration*

Abstract

The charge asymmetry in the production of top quark and antiquark pairs is measured in proton-proton collisions at a center-of-mass energy of 8 TeV. The data, corresponding to an integrated luminosity of $19.6\,\text{fb}^{-1}$, were collected by the CMS experiment at the LHC. Events with a single isolated electron or muon, and four or more jets, at least one of which is likely to have originated from hadronization of a bottom quark, are selected. A template technique is used to measure the asymmetry in the distribution of differences in the top quark and antiquark absolute rapidities. The measured asymmetry is $A_C^y = [0.33 \pm 0.26\,(\text{stat}) \pm 0.33\,(\text{syst})]\%$, which is the most precise result to date. The results are compared to calculations based on the standard model and on several beyond-the-standard-model scenarios.

Submitted to Physical Review D

*See Appendix A for the list of collaboration members

1 Introduction

The top quark is the heaviest particle in the standard model (SM) and the only fermion with a mass on the order of the electroweak scale [1]. Deviation of its production or decay properties from the SM predictions could signal physics beyond the SM. Several proposed extensions of the SM include heavy mediators of the strong interaction with axial coupling to quarks, collectively referred to as axigluons [2]. Top quark pair production in axigluon-mediated quark-antiquark annihilation can exhibit a forward-backward asymmetry that depends on the invariant mass of the system, similar to the asymmetry in fermion pair production mediated by Z bosons [3]. These types of models have been leading candidates for accommodating the behavior of $\mathrm{t\bar{t}}$ production in proton-antiproton collisions observed by FNAL Tevatron experiments based on about half of their full data set ($5\,\mathrm{fb}^{-1}$) [4, 5]. Since analyses of the full Tevatron data set ($10\,\mathrm{fb}^{-1}$) indicate smaller values of asymmetry [6, 7], and since recently improved SM-based theoretical calculations [8, 9] predict higher values of the asymmetry than previous calculations, the discrepancy between the SM and experimental observations has been greatly reduced. Measurements of dijet production [10–12] have constrained the range of axigluon masses and couplings [13], but the constraints are not applicable to models in which axigluon-produced dijet resonances are much broader than the experimental resolution, or which include multiparticle final states [14]. Precise measurement of the charge asymmetry in top quark pair production remains one of the best ways to test the limits of validity of SM predictions.

Experiments at the CERN LHC have reported values of charge asymmetry in top quark pair production [15–19] consistent with SM predictions [8, 9]. Corroboration of results from experiments at the Tevatron using measurements at the LHC is complicated by several differences between the two colliders. First, while at the Tevatron the majority of the $\mathrm{t\bar{t}}$ events are produced via quark-antiquark annihilation, at the LHC the $\mathrm{t\bar{t}}$ production is dominated by charge-symmetric gluon fusion, $\mathrm{gg} \to \mathrm{t\bar{t}}$. Second, collisions at the LHC are forward-backward symmetric, so observation of a charge asymmetry in $\mathrm{t\bar{t}}$ production via annihilation of a valence quark and a sea antiquark, $\mathrm{q\bar{q}} \to \mathrm{t\bar{t}}$, relies on the statistical expectation that the system be boosted in the direction of the quark momentum. Any difference in top quark and antiquark affinity for the initial quark or antiquark momentum will consequently result in more forward production of one and more central production of the other. This forward-central $\mathrm{t\bar{t}}$ charge asymmetry at the LHC is diluted relative to the forward-backward $\mathrm{t\bar{t}}$ charge asymmetry at the Tevatron since the LHC colliding system does not always have a boost in the expected direction. Third, a significant portion of LHC $\mathrm{t\bar{t}}$ events are due to (anti)quark-gluon initial states, qg ($\mathrm{\bar{q}g}$), which are charge asymmetric in number density as well as momentum, and which also contribute to the final-state forward-central $\mathrm{t\bar{t}}$ asymmetry. Despite these complications, the large number of $\mathrm{t\bar{t}}$ events produced at the LHC makes measurement of charge asymmetry competitive with the Tevatron measurements as a test of the SM.

The measurement of $\mathrm{t\bar{t}}$ asymmetry presented in this paper utilizes a template technique based on a parametrization of the SM. The technique differs from previous $\mathrm{t\bar{t}}$ asymmetry measurements [4–7, 15–19], which are based on unfolding the effects of selection and resolution in the observable distribution. Reference [19] in particular analyzes the same data set, but also differs in selecting fewer events with higher purity as a result of more restrictive jet transverse momentum criteria, and in the methods used to reconstruct $\mathrm{t\bar{t}}$ kinematics and determine the sample composition.

The template technique is presented in Section 2. Data from proton-proton collisions at $\sqrt{s} = 8\,\mathrm{TeV}$ were collected in 2012 by the CMS experiment, described in Section 3. Event selection, reconstruction of $\mathrm{t\bar{t}}$ kinematics, and a population discriminant are described in Section 4. The

details of the model used to obtain the result are given in Section 5, and the result is presented in Section 6. The analysis is summarized in Section 7.

2 Analysis strategy

Charge asymmetry in $\mathrm{t\bar{t}}$ production can be defined for an observable X that changes sign under the exchange $\mathrm{t} \leftrightarrow \bar{\mathrm{t}}$. If X is distributed with a differential cross section $\mathrm{d}\sigma/\mathrm{d}X$, its probability density is

$$\rho(X) = \frac{1}{\sigma}\frac{\mathrm{d}\sigma}{\mathrm{d}X}. \tag{1}$$

This can be expressed as a sum of symmetric (ρ^+) and antisymmetric (ρ^-) components,

$$\rho^{\pm}(X) = [\rho(X) \pm \rho(-X)]\,/2. \tag{2}$$

Statistical kinematic differences between top quarks and antiquarks can be summarized in a charge asymmetry,

$$A_c^X = \int_0^{\tilde{X}} \rho(X)\,\mathrm{d}X - \int_{-\tilde{X}}^0 \rho(X)\,\mathrm{d}X = 2\int_0^{\tilde{X}} \rho^-(X)\,\mathrm{d}X, \tag{3}$$

where the observable's maximum value $\tilde{X}$ may be finite or infinite. Previous LHC analyses [15–19] defined a $\mathrm{t\bar{t}}$ charge asymmetry A_c^y, based on the difference in absolute rapidities of the top quark (y_t) and antiquark ($y_{\bar{\mathrm{t}}}$),

$$\Delta|y|_{\mathrm{t\bar{t}}} = |y_\mathrm{t}| - |y_{\bar{\mathrm{t}}}|. \tag{4}$$

For the technique described in this paper, it is desirable that the observable X be bounded. The hyperbolic tangent is a symmetric and monotonic function, so the transformed observable

$$Y_{\mathrm{t\bar{t}}} = \tanh \Delta|y|_{\mathrm{t\bar{t}}}, \tag{5}$$

has the asymmetry A_c^y and is also bounded.

Charge asymmetries at production can only be determined from observed data distributions using an extrapolation based on a particular model. Past measurements were extrapolated using an unfolding technique, which relies on a model for the selection efficiencies and reconstruction effects [4–7, 15–19]. An alternative extrapolation discussed in this paper uses a model to derive template distributions for the symmetric and antisymmetric components, $\rho^{\pm}$.

In the present analysis, the next-to-leading-order (NLO) POWHEG event generator (version 1.0) [20] is used in association with the CT10 [21] parton distribution functions (PDFs) as a base model to construct the symmetric and antisymmetric components of the probability density $\rho(X)$ for an observable X. These distributions are represented as symmetrically binned histograms, given as vectors $\vec{x}^{\pm}$ with a dimensionality equal to the number of bins. A generalized model with a single parameter α can be constructed from a linear combination of the base model components,

$$\vec{x}^{\alpha} = \vec{x}^{+} + \alpha\vec{x}^{-}. \tag{6}$$

The measurement strategy is to find the value of α that best fits the observations. The base model charge asymmetry $\hat{A}_c^X$ is given by Eq. (3). The charge asymmetry observed in data is then equal to that of the base model scaled by the parameter α:

$$A_c^X(\alpha) = \alpha\hat{A}_c^X. \tag{7}$$

Table 1: The $\mathrm{t\bar{t}}$ initial-state fractions and charge asymmetries in the observable $Y_{\mathrm{t\bar{t}}}$, calculated with POWHEG using the CT10 PDFs. The statistical uncertainty in the last digit is indicated in parentheses.

Initial state	Fraction (%)	$\hat{A}_c^y$ (%)
gg	65.2	−0.06(3)
$\mathrm{q\bar{q}}$	13.4	2.95(6)
qg	18.2	1.17(5)
$\mathrm{\bar{q}g}$	3.2	−0.2(1)
pp	100.0	0.56(2)

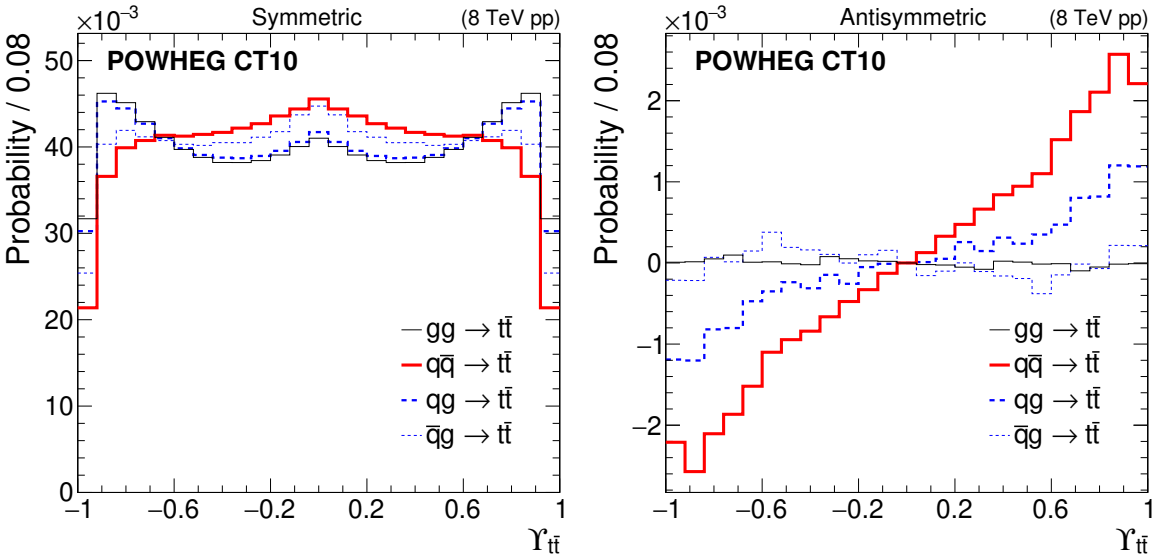

Figure 1: The (left) symmetric $\vec{x}^{+}$ and (right) antisymmetric $\vec{x}^{-}$ components of the binned probability distributions in the observable $Y_{\mathrm{t\bar{t}}}$, constructed using POWHEG [20] with CT10 PDFs [21], for $\mathrm{t\bar{t}}$ production from gg, $\mathrm{q\bar{q}}$, qg, and $\mathrm{\bar{q}g}$ initial states.

Figure 1 presents the $\vec{x}^{\pm}$ distributions in gg, $\mathrm{q\bar{q}}$, and qg ($\mathrm{\bar{q}g}$) initial states for $X = Y_{\mathrm{t\bar{t}}}$, before the event reconstruction and selection are applied, and the composition and intrinsic charge asymmetries of each initial state are listed in Table 1. Imperfect detector resolution, event reconstruction, and selections can result in distributions of the reconstructed observable $Y_{\mathrm{t\bar{t}}}^{\mathrm{rec}}$ that differ from those in $Y_{\mathrm{t\bar{t}}}$. For this reason, the symmetric and antisymmetric templates, $\vec{x}_{\mathrm{rec}}^{\pm}$, are constructed using POWHEG-generated events that are fully reconstructed and pass the selection criteria. Studies of simulated events show that there is no significant constant bias in the charge asymmetry caused by event reconstruction and selection. Thus, the scale parameter α in Eqs. (6, 7) can be determined by a fit to the reconstructed distribution in data,

$$\vec{x}_{\mathrm{data}}^{\alpha} = \vec{x}_{\mathrm{rec}}^{+} + \alpha \vec{x}_{\mathrm{rec}}^{-}. \tag{8}$$

3 CMS detector and definition of physics objects

The central feature of the CMS apparatus is a superconducting solenoid of 6 m internal diameter, providing a magnetic field of 3.8 T. Within the solenoid volume are a silicon pixel and strip tracker, a lead tungstate crystal electromagnetic calorimeter (ECAL), and a brass and scintillator hadron calorimeter (HCAL), each composed of a barrel and two endcap sections. Muons are measured in gas-ionization detectors embedded in the steel flux-return yoke outside the

solenoid. Extensive forward calorimetry complements the coverage provided by the barrel and endcap detectors.

The first level of the CMS trigger system, composed of custom hardware processors, uses information from the calorimeters and muon detectors to select the most interesting events in a fixed time interval of less than 4 μs. The high-level trigger processor farm further decreases the event rate from around 100 kHz to around 400 Hz, before data storage. Single-electron and single-muon triggers were used to collect events for this analysis.

The particle-flow event algorithm [22, 23] is used to reconstruct and identify each individual particle with an optimized combination of information from the various elements of the CMS detector. Photons and electrons are defined as clusters in ECAL with a requirement that there be a charged-particle trajectory pointing to an electron cluster. The energy of a photon is directly obtained from the ECAL measurement, corrected for zero-suppression effects. The energy of an electron is determined from a combination of the electron momentum at the primary interaction vertex as determined by the tracker, the energy of the corresponding ECAL cluster, and the energy sum of all bremsstrahlung photons spatially compatible with originating from the electron track [24]. The momentum of a muon is obtained from the direction and curvature of its combined trajectory in the muon and tracking systems. The energy of a charged hadron is determined from a combination of its momentum measured in the tracker and the matching ECAL and HCAL energy deposits, corrected for zero-suppression effects and for the response function of the calorimeters to hadronic showers. Finally, the energy of a neutral hadron is obtained from the corresponding corrected ECAL and HCAL energy deposits.

For each event, after identification and removal of leptons relevant to the sample selection and particles from additional proton-proton interactions within the same bunch crossing (pileup), hadronic jets are clustered from these reconstructed particles with the infrared- and collinear-safe anti-k_{T} algorithm, operated with a size parameter R of 0.5 [25]. The jet momentum is determined as the vectorial sum of all particle momenta in this jet, and is found in the simulation to be within 5 to 10% of the true momentum over the whole transverse momentum (p_{T}) spectrum and detector acceptance. Jet energy corrections are derived from the simulation, and are confirmed with in situ measurements of the energy balance of dijet and photon+jet events [26]. The jet energy resolution amounts typically to 15% at 10 GeV, 8% at 100 GeV, and 4% at 1 TeV. An offset correction is applied to jet energies to take into account pileup contributions. Additional selection criteria are applied to each event to remove spurious jet-like features originating from isolated noise patterns in certain HCAL regions. Jets from b quarks are identified using a discriminant containing information about secondary vertices formed by at least three charged-particle tracks, including the number of associated tracks, the displacement from the collision point, and the vertex mass, which is computed from the tracks associated with the secondary vertex [27].

The missing transverse momentum vector $\vec{p}_{\mathrm{T}}^{\,\mathrm{miss}}$ is defined as the projection on the plane perpendicular to the beams of the negative vector sum of the momenta of all reconstructed particles in an event. Its magnitude is referred to as $E_{\mathrm{T}}^{\mathrm{miss}}$.

A more detailed description of the CMS detector, together with a definition of the coordinate system used and the relevant kinematic variables, can be found in Ref. [28].

4 Event selection and reconstruction

Each event is considered under the hypothesis that a top quark and a top antiquark each decay into a bottom quark and a W boson, and that one W boson subsequently decays into a pair of quarks, while the other decays into a neutrino and either an electron or a muon, producing a lepton and jets (ℓ+jets) signature.

Events are selected from data collected from collisions of protons at 8 TeV center-of-mass energy and corresponding to an integrated luminosity of $(19.6 \pm 0.5)\,\text{fb}^{-1}$ [29]. Selected events contain at least four jets each with $|\eta| < 2.5$ and $p_\text{T} > 20\,\text{GeV}$, one isolated electron (muon) with $|\eta| < 2.5$ (2.1) and $p_\text{T} > 30$ (26) GeV. Events are also required to have no other electrons ($|\eta| < 2.5$, $p_\text{T} > 20\,\text{GeV}$) or muons ($|\eta| < 2.5$, $p_\text{T} > 10\,\text{GeV}$). A selected event must have an electron with a particle-flow relative isolation I^rel_PF less than 0.1, or a muon with I^rel_PF less than 0.12 [24, 30]. Events containing an electron with $0.11 < I^\text{rel}_\text{PF} < 0.15$ or a muon with $0.13 < I^\text{rel}_\text{PF} < 0.20$ are retained as a control, or sideband, region. The (next-to-) leading jet must have $p_\text{T} > 45$ (35) GeV. At least one jet must be b-tagged, as defined by the medium working point of the combined secondary vertex b tagging discriminant (CSV), which has an efficiency better than about 65% and a misidentification probability of about 1.5% [27]. In total, 326 185 events are accepted with an electron and jets in the final state, hereafter referred to as the e+jets channel, and 340 911 events are accepted in the μ+jets channel.

In addition to $\mathrm{t\bar{t}}$ production, several other processes can produce a ℓ+jets signature that passes this selection. In particular, these processes include production of leptonically decaying W bosons in association with jets (Wj), Drell–Yan (DY) production of $\ell^+\ell^-$ pairs from $\mathrm{q\bar{q}}$ annihilation in association with jets and in which one lepton is not identified, and the production of single top (St) quarks accompanied by additional jets. Production of quantum chromodynamic multijets (Mj) also contributes to the background. Such events can satisfy the selection if a jet is misidentified as an electron or if a muon produced in the decay of a heavy quark passes the isolation criteria.

More than 65% of selected events contain $\mathrm{t\bar{t}}$ pairs.

4.1 Modeling of signal and background

The detection of generated particles is fully simulated with the GEANT4 software [31] using a detailed description of the CMS detector. The samples account for the observed multiplicity of pileup interactions in data. Additional weights are applied after event selection to match the efficiency of triggers and object identification that are measured in a data sample of Z+jets events using a tag-and-probe method [24, 30]. The energy difference between each reconstructed jet and its corresponding generated jet is scaled to match the (η- and p_T-dependent) jet energy resolution in data, as measured using the dijet asymmetry technique [26].

As mentioned, the $\mathrm{t\bar{t}}$ events are generated with the NLO POWHEG heavy-quark pair production algorithm, using the CT10 PDFs, and interfaced with PYTHIA (version 6.426) for parton showering and hadronization [32–34]. Events with W or Z bosons in conjunction with 1, 2, 3, or 4 jets are generated with leading-order (LO) MADGRAPH (version 5.1.3.30) [35], also interfaced with PYTHIA. A dedicated W+$\mathrm{b\bar{b}}$ sample is used for investigation of systematic uncertainties. Events with single top quarks or antiquarks are generated with POWHEG in the s and t channels [36], and are generated in the tW channel using diagram removal rather than the diagram subtraction method [37].

The Mj background has a very low efficiency to pass the selection, making it difficult to simulate enough selected events, but it has a large enough cross section to make it significant. The Mj

background is modeled using the sideband data, subtracting the contributions of simulated processes, which are normalized according to the integrated luminosity and their cross sections and selection efficiencies.

Several alternative models of $\mathrm{t\bar{t}}$ production are used to investigate systematic uncertainties and to evaluate the performance of the method. Alternative SM $\mathrm{t\bar{t}}$ simulations are generated with MADGRAPH and with MC@NLO (version 3.41) [38] using the CTEQ6 PDFs (versions L1 and M, respectively) [39]. Systematic uncertainties related to the factorization and renormalization scales are evaluated using POWHEG $\mathrm{t\bar{t}}$ samples in which both scales are increased or decreased simultaneously by a factor of two from their nominal values, equal to the event momentum transfer squared; these control samples are processed with the FASTSIM [40] simulation of the CMS detector. A set of six models in which $\mathrm{t\bar{t}}$ production kinematics are modified by the presence of new physics are generated with MADGRAPH, and are described in detail in Ref. [13]. The models are chosen to have parameters not yet excluded by other experimental constraints. The set includes a model with an added complex gauge boson Z' [41] with a mass of 220 GeV and a coupling to right-handed up-type quarks. Other models in the set include parametrized color-octet vector bosons (axigluon) models [2], in which the axigluon has nonzero mass and chiral couplings. Three models include a light axigluon with a 200 GeV mass and coupling characterized as right, left, or axial. Two models include a heavy axigluon with a 2 TeV mass and right or axial coupling.

4.2 Reconstruction of top quarks

Top quarks are reconstructed using the most likely assignment of the reconstructed jets to the $\mathrm{t\bar{t}}$ decay partons. Jet four-momenta are corrected according to their parton assignment and a kinematic fit, which uses the known top quark and W boson masses [1]. The neutrino momentum is calculated analytically [42]. The top quark and antiquark four-momenta are found by summing the four-momenta of their respective decay products. The charge of the leptonically decaying top quark is determined by that of the electron or muon, while the top quark that decays into jets is assumed to be of the opposite charge.

All jet assignments are considered in selecting the assignment of maximum likelihood. The selection ensures that the number of jets in the event N_j is at least four. There are $N_c = \frac{1}{2}N_j!/(N_j-4)!$, or a minimum of 12, possible jet assignment combinations. Each assignment is represented by a tuple $(a, b, c, d, \{x\})$, where a represents the b jet associated with $\mathrm{t} \to \mathrm{b}\ell\nu_\ell$ decay, b represents the b jet associated with $\mathrm{t} \to \mathrm{bq\bar{q}}$ decay, c and d represent the two jets from hadronic W boson decay, ordered by p_T, and $\{x\}$ represents any additional jets in the event, ordered by p_T. The correct assignment in simulation is designated $(\hat{a}, \hat{b}, \hat{c}, \hat{d}, \{\hat{x}\})$.

The scale factors for correcting the energy of the jets from the reconstruction to the parton level are obtained from $\mathrm{t\bar{t}}$ simulation, following the event selection, for b jets from top quark decay, jets from W boson decay, and other jets. Corrections are found as a function of p_T in three bins of absolute pseudorapidity, with upper bin boundaries at $|\eta| = 1.131$, 1.653, and 2.510, corresponding to the calorimeter barrel, transition, and endcap regions. The corrections, shown in Fig. 2, are applied to the measured jet energies according to the assignment.

The likelihood of a given jet-to-parton assignment i is

$$L_i = L_i^{\mathrm{CSV}}\, LR_i^{\mathrm{MSD}}\, LR_i^{\chi}, \tag{9}$$

where L_i^{CSV} is the likelihood of the jet b tagging discriminants, LR_i^{MSD} is the likelihood ratio of the invariant masses of jet combinations associated with $\mathrm{t} \to \mathrm{bq\bar{q}}$ decays, and LR_i^{χ} is the likelihood ratio of the χ^2 associated with the products from $\mathrm{t} \to \mathrm{b}\ell\nu_\ell$ decays.

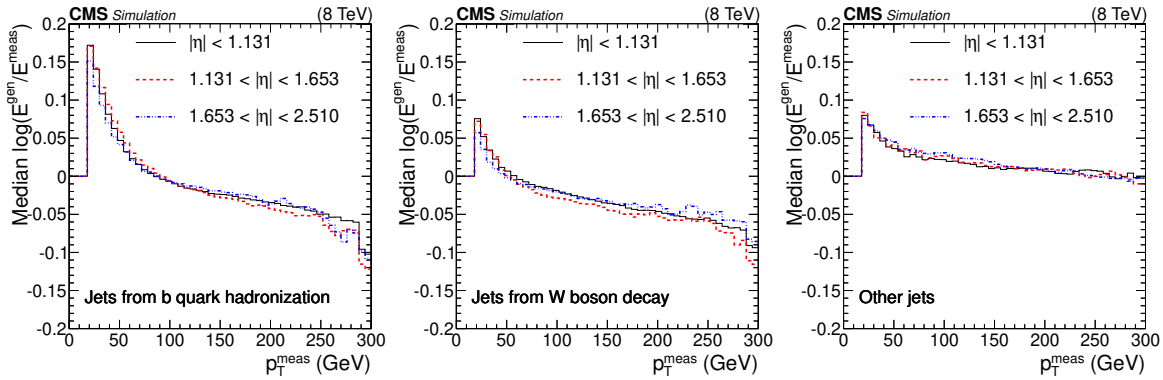

Figure 2: The median value of the logarithm of the ratio of parton energy to measured energy, as a function of measured p_{T} in three bins of $|\eta|$, for (left) b jets from top quark decay, (center) jets from W boson decay, and (right) other jets.

The CSV b tagging discriminant associates a value β with each jet. The conditional CSV probability densities $\mathcal{B} = \rho(\beta|\hat{a},\hat{b})$, $\mathcal{Q} = \rho(\beta|\hat{c},\hat{d})$, and $\mathcal{N} = \rho(\beta|\{\hat{x}\})$ are shown in Fig. 3. The likelihood of a given jet assignment i, considering the associated CSV values $\{\beta\}$, is

$$L_i^{\mathrm{CSV}} = \mathcal{B}(\beta_a)\mathcal{B}(\beta_b)\mathcal{Q}(\beta_c)\mathcal{Q}(\beta_d) \prod_{j\in\{x\}} \mathcal{N}(\beta_j). \tag{10}$$

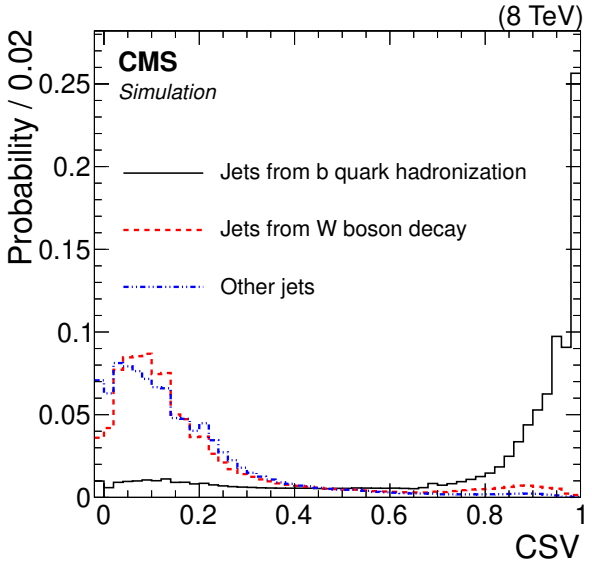

Figure 3: The conditional probability densities of the CSV b tagging discriminant from simulation for jets from b quarks, jets from W boson decay, and other jets.

The jet invariant masses associated with $\mathrm{t} \to \mathrm{bq\bar{q}}$ decays are m_{bcd} and m_{cd}, with parton-level jet corrections applied based on the assignment. Their two-dimensional probability distribution for correct assignments is shown in Fig. 4. The mean and variance of this distribution are calculated after removing the tail of the distribution, defined as the lowest-valued bins which integrate to a 1% probability, in order to find a Gaussian approximation. Contours of the approximation, in standard deviations, are also shown in Fig. 4. The distance of a point from the center of this Gaussian function, expressed in units of standard deviations, is denoted by "mass standard deviations" (MSD). Probability distributions in MSD for correct and incorrect assignments, and their ratio LR^{MSD}, are shown in Fig. 4.

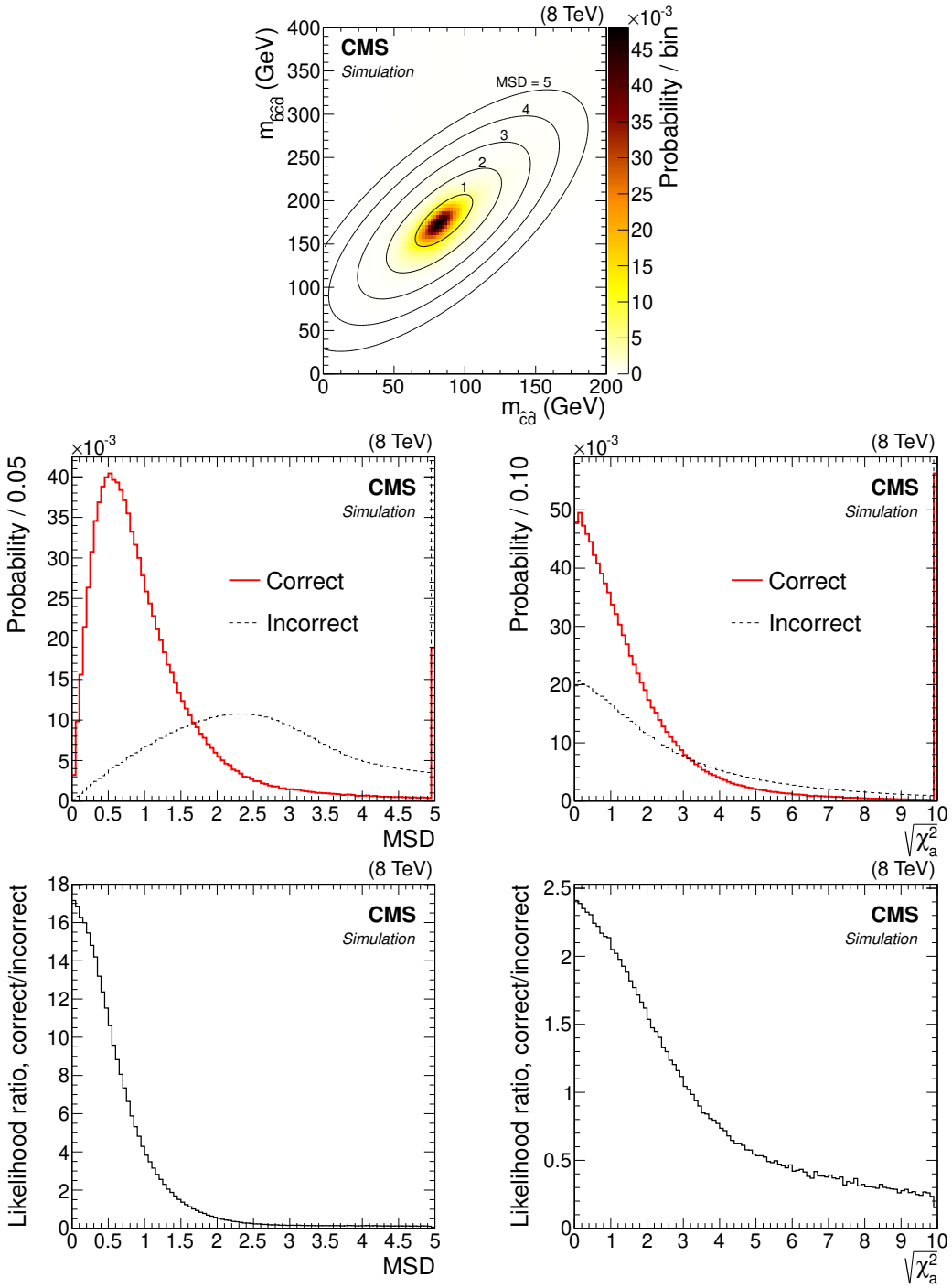

Figure 4: The two-dimensional probability density from simulation of jet invariant masses from W boson ($m_{\hat{c}\hat{d}}$) and top quark ($m_{\hat{b}\hat{c}\hat{d}}$) decay is shown (top), along with contours in standard deviations (MSD) of the corresponding Gaussian approximation. Probability densities for correct and incorrect jet assignments (middle) are shown (left) for MSD and (right) for $\sqrt{\chi^2_a}$ of the leptonically decaying top quark reconstruction. The corresponding likelihood ratios are shown below.

The momentum of the neutrino associated with the leptonically decaying top quark is calculated according to Ref. [42] using $\vec{p}_{\mathrm{T}}^{\,\mathrm{miss}}$ and the four-momenta of the charged lepton and jet a. Correct and incorrect assignments of jet a are discriminated using the test statistic

$$\chi_a^2 = \mathbf{d}^T \sigma^{-2} \mathbf{d}, \tag{11}$$

where σ^2 is the covariance matrix for $\vec{p}_{\mathrm{T}}^{\,\mathrm{miss}}$, derived from the momentum uncertainties of the reconstructed objects in the event, and $\mathbf{d}$ is the difference vector in the transverse plane between $\vec{p}_{\mathrm{T}}^{\,\mathrm{miss}}$ and the neutrino momentum solution. The distributions of the square root of χ_a^2 for correct and incorrect assignments of jet a, and their ratio LR^{χ}, are shown in Fig. 4.

Of the selected $\mathrm{t\bar{t}}$ events, about half contain reconstructed jets corresponding to all four $\mathrm{t\bar{t}}$ decay partons. In about 60% of those events, the assignment with the maximum likelihood is also the correct assignment.

4.2.1 Kinematic fitting procedure

The energy resolution of jets corresponding to the most probable assignment can be improved beyond the intrinsic resolution of the CMS detector using the constraints from the masses of the top quark and W boson. These constraints are applied in two stages. First, jet four-momenta p_i are scaled to $\hat{p}_i = (1+\delta_i)p_i$ with the free parameters δ_i, for i equal to b, c, or d, in the minimization of the test statistic

$$\chi^2_{bcd} = \left(\frac{m_{\mathrm{W}} - \hat{m}_{cd}}{\Gamma_{\mathrm{W}}/2}\right)^2 + \left(\frac{m_{\mathrm{t}} - \hat{m}_{bcd}}{\Gamma_{\mathrm{t}}/2}\right)^2 + \sum_{i=bcd}\left(\frac{\delta_i}{r_i}\right)^2. \tag{12}$$

Here, r_i are the p_{T}- and η-dependent relative jet energy resolutions σ_E/E, and $\hat{m}_{cd}$ and $\hat{m}_{bcd}$ are the invariant masses calculated with the scaled jet four-momenta. The mass and width parameters used for the W boson and top quark are: $m_{\mathrm{W}} = 80.4\,\mathrm{GeV}$; $m_{\mathrm{t}} = 172.0\,\mathrm{GeV}$; $\Gamma_{\mathrm{W}} = 2\,\mathrm{GeV}$; and $\Gamma_{\mathrm{t}} = 13\,\mathrm{GeV}$. The values of Γ_{t} and Γ_W represent the empirical resolution of the reconstructed particle masses for a single event, rather than the natural particle widths. The momentum and energy of the top quark that decays into jets are given by $\sum_{\{bcd\}}\hat{p}_i$. In the second stage, the four-momentum of jet a is scaled to $\hat{p}_a = (1+\delta_a)p_a$ with the free parameter δ_a, to minimize the test statistic χ_a^2 from Eq. (11). At each step of this minimization, χ_a^2 is calculated with the charged-lepton four-momentum, the candidate $\hat{p}_a$, and $\vec{p}_{\mathrm{T}}^{\,\mathrm{miss}}$ corrected for the scaling of the a, b, c, and d jets. The uncertainty in the corrected $\vec{p}_{\mathrm{T}}^{\,\mathrm{miss}}$ is reduced from that of the nominal reconstruction by removing a portion of the uncertainty corresponding to the energies of the a, b, c, and d jets. The neutrino momentum associated with the minimized χ_a^2 is summed with the corresponding $\hat{p}_a$ and the charged lepton four-momentum to find the energy and momentum of the leptonically decaying top quark.

4.3 Discrimination among three populations

To measure the sample composition in the data after the event selection, we construct a likelihood discriminant designed to distinguish among populations of events from three leading processes: $\mathrm{t\bar{t}}$, Mj, and Wj, denoted respectively by P_1, P_2, and P_3 in the following generalized construction. As will be discussed in Section 5, the contributions from St and DY are constrained to those predicted by their SM cross sections. The likelihood that an event belongs to population P is $L_P = \prod_i \ell_i^P(V_i)$, where $\{V_i\}$ is a set of random variables with probability densities ℓ_i^P. For independent $\{V_i\}$, the likelihood ratio L_{P_2}/L_{P_1} is more discriminating than any single constituent variable [43]. One can construct a likelihood-ratio-based discriminant

$$\Delta = \mathrm{Arg}\left(L_{P_1} + \mathrm{e}^{2i\pi/3}L_{P_2} + \mathrm{e}^{-2i\pi/3}L_{P_3}\right)/\pi, \tag{13}$$

the principal value of which is bounded periodically on (-1,1] and is symmetric under exchange of any two of the three populations. Figure 5 illustrates the construction. Populations P_1, P_2, and P_3 tend to concentrate at Δ of 0, $2/3$, and $-2/3$, respectively.

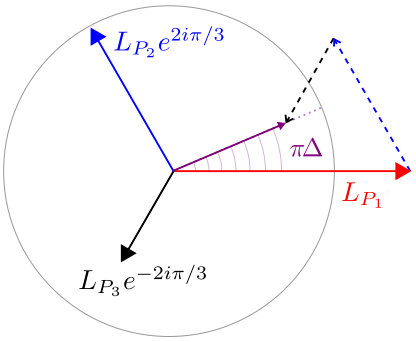

Figure 5: The angle $\pi\Delta$ of the resultant sum of three vectors spaced at equal angles, in which the magnitude of each is the likelihood of the respective population. The dashed arrows are translations of the $e^{2i\pi/3}$ and $e^{-2i\pi/3}$ vectors which illustrate the construction of the sum. The circle is shown to indicate the relative scale.

Three observables are used to construct the likelihoods for the discriminant. The first is the transverse mass $M_T = \sqrt{2\ell_T E_T^{miss}(1-\cos\phi)}$, where ℓ_T is the magnitude of the charged lepton p_T, ϕ is the azimuthal angle between the charged lepton momentum and $\vec{p}_T^{miss}$, and E_T^{miss} is the magnitude of $\vec{p}_T^{miss}$. The second is the probability from the MSD that at least one jet assignment is the correct one, defined as $P_{MSD} = \sum LR_i^{MSD} / \left(N_c + \sum LR_i^{MSD}\right)$, where N_c and LR_i^{MSD} are defined in Section 4.2. The third is the probability from the CSV b tagging discriminant that at least one jet assignment is the correct one, defined as

$$P_{CSV} = \frac{\epsilon \sum L_i^{CSV}}{\epsilon \sum L_i^{CSV} + (1-\epsilon) N_c \prod_{j\in\{jets\}} \mathcal{N}(\beta_j)}, \tag{14}$$

where L_i^{CSV} and $\mathcal{N}$ are defined in and before Eq. (10), and the prior probability that at least one assignment is correct is set to $\epsilon = 0.05$. A value of $\epsilon = 0.05$ is chosen because it results in a more balanced distribution of P_{CSV} than, for example, a flat prior with $\epsilon = 0.5$. We found these observables to be highly discriminating and mostly independent of each other.

The probability distribution for each population is shown as a function of the discriminant and each of its input observables in Fig. 6. The Mj probability distributions for the inputs are calculated using fixed SM cross sections, as determined by the simulations, for the subtracted $t\bar{t}$ and Wj contributions.

5 Measurement procedure

A two-stage maximum-likelihood fit is employed to sequentially measure the sample composition, using the Δ distribution, and the charge asymmetry, using the $Y_{t\bar{t}}^{rec}$ distribution.

The sample composition is determined independently for each lepton channel by fitting a model to the observed distribution N_i^ℓ in the discriminant Δ. Normalized five-bin templates in Δ are constructed from the selected events for each of the simulated processes, including $t\bar{t}$, Wj, St, and DY, in both the signal and sideband regions. The total number of events expected in each region from simulated process j is the product of the integrated luminosity $\mathcal{L}$, the cross

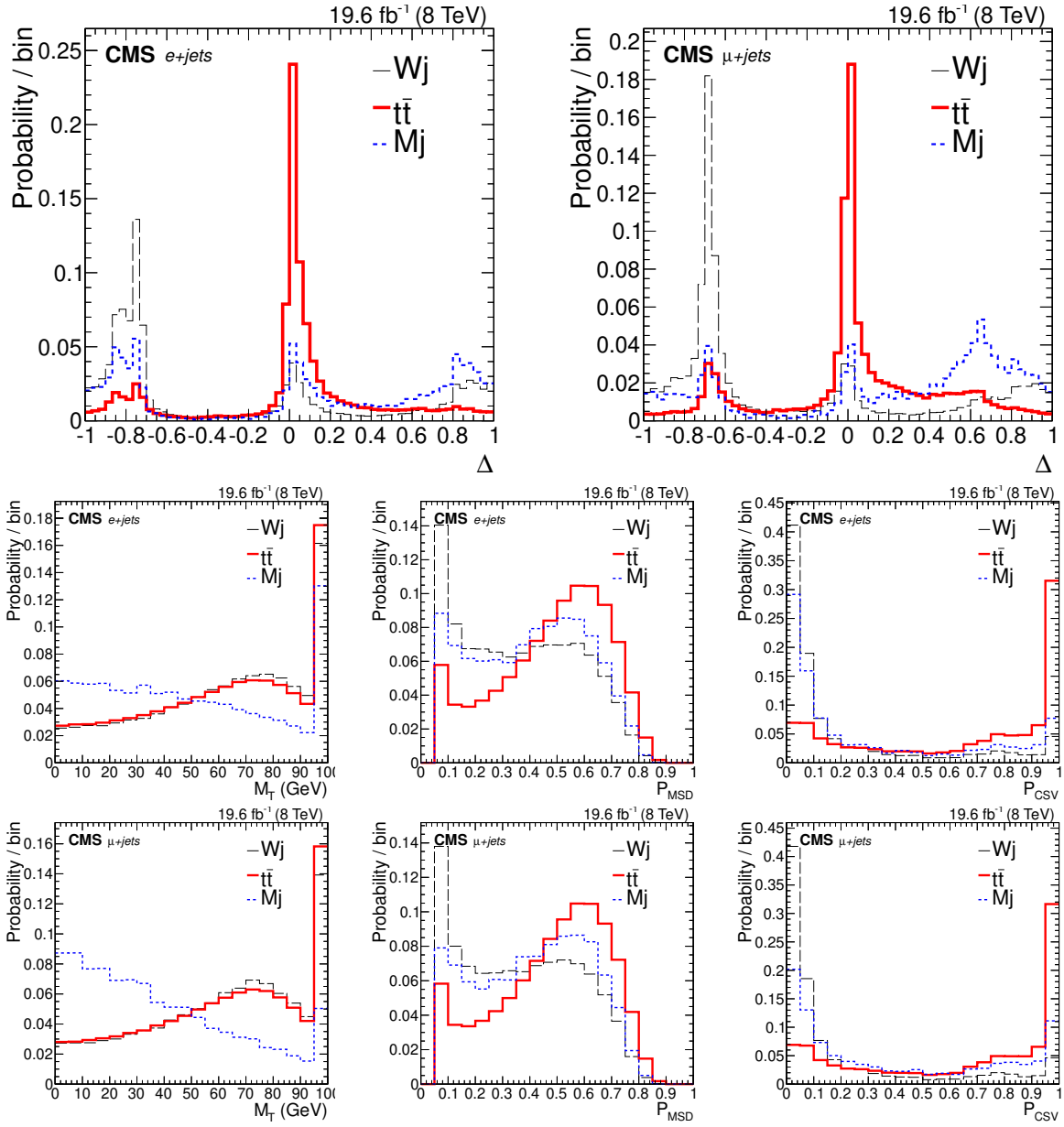

Figure 6: The probability distribution of the discriminant Δ for (top left) selected e+jets events and (top right) selected μ+jets events, for the simulated Wj and $t\bar{t}$ populations, and for the Mj population, which is modeled from the sideband data with simulated contributions subtracted. The probability distributions in each observable used to construct the discriminant are shown for (middle) e+jets and (bottom) μ+jets channels. The overflow is included in the rightmost bin of the M_T distributions.

section σ_j, and the selection efficiency. The selection efficiencies are taken directly from simulation. Each cross section is parametrized by the relative change δ_j from the nominal value $\hat{\sigma}_j$. The integrated luminosity is parametrized by the relative change $\delta_{\mathcal{L}}$ from the measured central value. The Mj distribution in Δ is determined at each iteration of the fit by subtracting the sideband contributions of simulated processes from the sideband region in data, and then rescaling this distribution by a positive parameter F^{ℓ}_{Mj}. The total number of expected events in each bin, λ^{ℓ}_i, is the sum of the expected contributions from the $\mathrm{t\bar{t}}$, Wj, Mj, St, and DY processes. Parameters $\delta_{\mathcal{L}}$, δ_{St}, and δ_{DY} are held fixed to zero or to nonzero values when investigating systematic uncertainties. The sample composition is determined by finding values of the free parameters $\{F^{e}_{\mathrm{Mj}}, F^{\mu}_{\mathrm{Mj}}, \delta_{\mathrm{t\bar{t}}}, \delta_{\mathrm{Wj}}\}$ that maximize the product of the Poisson likelihoods over the bins, given observations N^{ℓ}_i and expectations λ^{ℓ}_i. The fit is implemented using RooFit [44].

The charge asymmetry is determined from a fit to the five-bin distribution in $Y^{\mathrm{rec}}_{\mathrm{t\bar{t}}}$, based on the same model. With the sample composition parameters held fixed, and following Eq. (8), the POWHEG $\mathrm{t\bar{t}}$ model is extended by introducing a new free parameter α to provide changes in the relative magnitudes of the symmetric and antisymmetric components of $Y^{\mathrm{rec}}_{\mathrm{t\bar{t}}}$, shown in Fig. 7. The difference in shape of the e+jets and μ+jets templates is a result of the different rapidity coverage between the two lepton flavors. The modeled charge asymmetry is that of the $\mathrm{t\bar{t}}$ base model, $\hat{A}^{y}_{c}$, scaled by α,

$$A^{y}_{c} = \alpha \hat{A}^{y}_{c}. \tag{15}$$

The charge asymmetry in the data is estimated by finding the value of α that maximizes the product of the Poisson likelihoods over the bins. The results from the independent measurements in both lepton channels are combined before evaluating the systematic uncertainties.

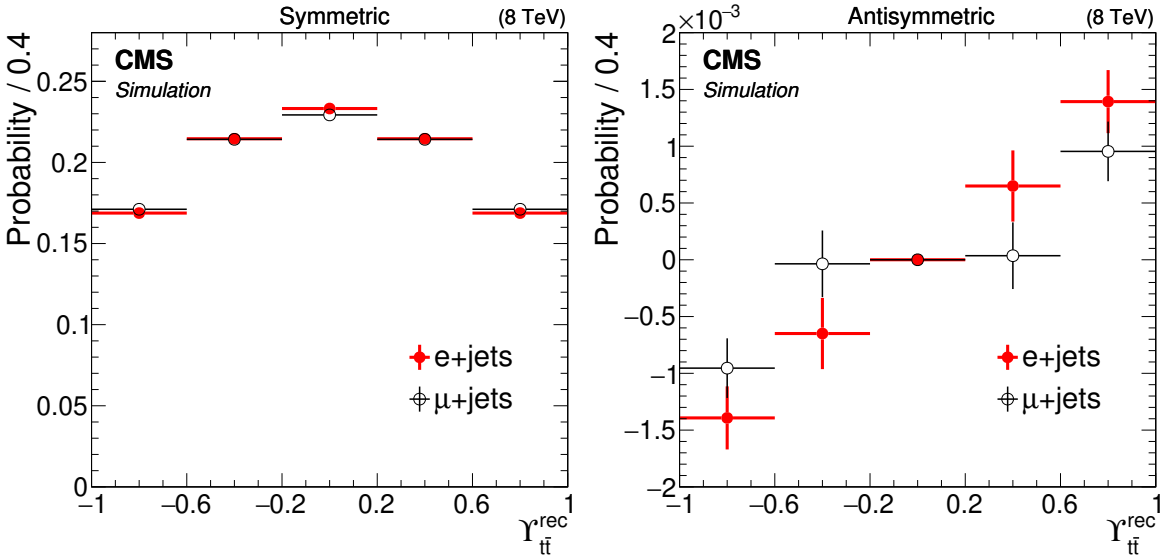

Figure 7: The (left) symmetric and (right) antisymmetric components of the $Y^{\mathrm{rec}}_{\mathrm{t\bar{t}}}$ probability distribution for selected $\mathrm{t\bar{t}}$ simulation events in the e+jets and μ+jets channels. The vertical bars show the statistical uncertainties, while the horizontal bars display the bin widths.

5.1 Performance and calibration

The performance of the method is checked on simulated samples constructed using $\mathrm{t\bar{t}}$ events based on the extended POWHEG model as well as the alternative $\mathrm{t\bar{t}}$ simulations described in

Section 4.1. The extended POWHEG model is checked using various values of the parameter α by measuring pseudo-experiments generated with Poisson variations of the best-fit model, mimicking fluctuations expected in data. The statistical uncertainty measured in 68% of the pseudo-experiments is greater than the absolute difference between the measured and expected values. The distribution in statistical uncertainty in A_c^y, with an expected value of 0.258%, is shown in Fig. 8.

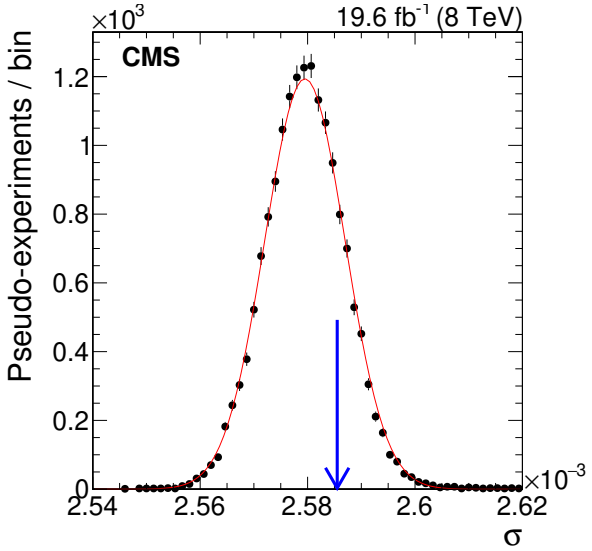

Figure 8: The distribution of the statistical uncertainty in A_c^y from measurements using pseudo-experiments, with an expected value of 0.258%. The statistical uncertainty extracted from the data is marked by the arrow.

The alternative $t\bar{t}$ simulations are checked using pseudo-experiments with the sample composition of the measured data, constructed with fixed background and Poisson-varied signal templates, to find the uncertainty from the sample statistics of each alternative model. Figure 9 shows the difference between the expected measurement and the input charge asymmetries, or the bias, for each model. The bias for the extended POWHEG models is negligible. The bias of the method when applied to samples produced using the SM-based generators MADGRAPH and MC@NLO is compatible with the systematic uncertainty in A_c^y assigned to model-related sources, represented by the shaded band in the plot. Model-related systematic uncertainty sources consist of simulation statistics, modeling of $t\bar{t}$ production, PDFs, and renormalization and factorization scales. Similar calibrations of the beyond-SM alternatives of $t\bar{t}$ production considered in this study all show biases statistically compatible with zero.

5.2 Systematic uncertainties

Systematic uncertainties in α are investigated after the statistical combination of the two channels by repeating the measurement with variations in the parameters or the distributions. The second stage of the fit is repeated with sample composition parameters varied independently to the upper and lower bounds of their 68% confidence intervals. Parameters for the integrated luminosity and the St and DY cross sections are varied similarly, but both fit stages are repeated. The effects of statistical uncertainty in the sideband distributions of the data and the simulations are investigated with ensembles of alternative templates, generated by varying the originals according to Poisson statistics. Uncertainty in the jet energy scale and jet energy resolutions are investigated by repeating the reconstruction using rescaled jet energies, according

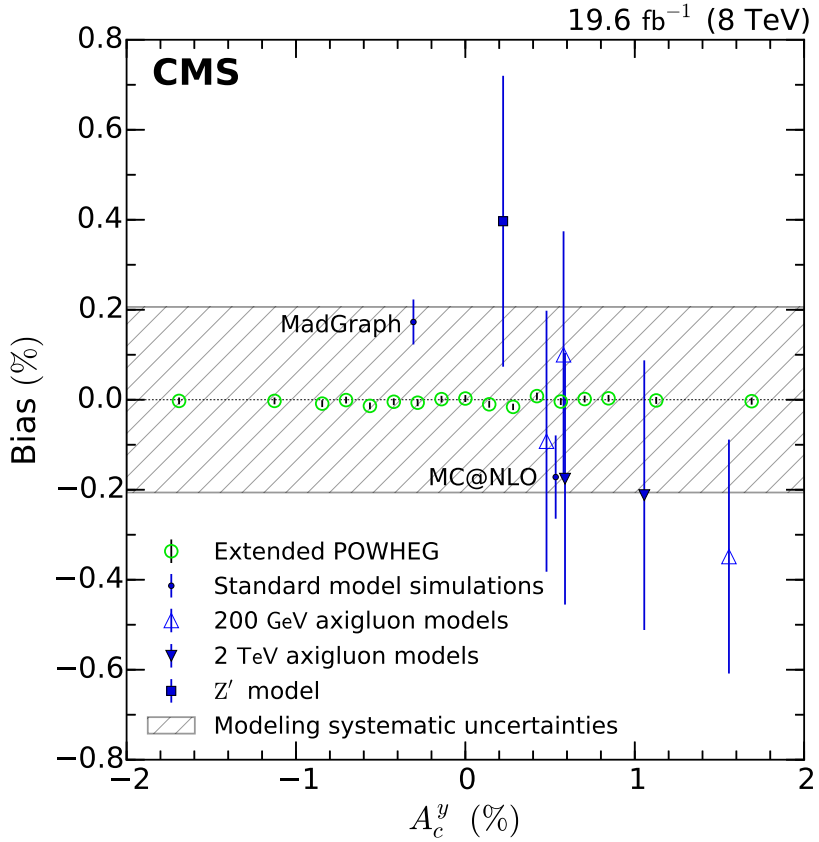

Figure 9: The bias in the measured charge asymmetry for SM simulations and alternative $t\bar{t}$ models, based on extended POWHEG SM templates, versus the charge asymmetry in each sample. The beyond-SM samples are MADGRAPH simulations of Z′ bosons and axigluons with masses of 200 GeV and 2 TeV. Uncertainty in the bias of the extended POWHEG model is dominated by the number of pseudo-experiments used, while the uncertainty in the bias of each alternative model is dominated by the statistical uncertainty in the sample. The hatched area shows the systematic uncertainty in the measurement of A_c^y assigned to the modeling.

to the p_T and η of each jet. Likewise, the modeling of the b tagging discriminator is varied by repeating the reconstruction with scaled discriminant values. The PDFs are varied by event reweighting of the $t\bar{t}$ templates to the 90% confidence limits of each of the 26 CT10 eigenvectors and the strong coupling parameter, independently; this method is more conservative than the widely used PDF4LHC prescription [45] since it is sensitive to the possibility of a strong correlation between the antisymmetric component of the $Y_{t\bar{t}}^{rec}$ distribution and any eigenvector, while varying the distribution to the minimum and maximum of the uncertainty envelope is not. Uncertainty from the modeling of $t\bar{t}$ production is estimated by measuring the data using extended MC@NLO templates rather than the extended POWHEG templates, and varying the top quark mass by ± 0.9 GeV. The factorization and renormalization scales are varied by substituting distinct samples for the $t\bar{t}$ templates, described in Section 4.1. The heavy-flavor content of Wj events is varied by adding or subtracting 20% of the expected contribution of a distinct W+$b\bar{b}$ sample to the expected Wj templates. Variations in distributions for the pileup multiplicity and the top quark p_T, and variations in the trigger and identification efficiencies for the charged leptons, are accomplished by event reweighting. The uncertainty in the shape of the Mj templates is dominated by the statistical uncertainty in the data sidebands; the Mj antisymmetric components are statistically compatible with zero asymmetry, and no additional shape systematic is included beyond that of the statistical shape uncertainty.

The magnitudes of the systematic uncertainties are given in Table 2. The total systematic uncertainty of 0.33% is comparable to the statistical uncertainty in the measurement, and is dominated by the statistical uncertainty in the shapes of the data sidebands.

Table 2: Uncertainty in the combined measurement of A_c^y from systematic sources, ordered by decreasing magnitude.

(%)	Source of systematic uncertainty in A_c^y
0.18	Data sideband statistical uncertainty
0.15	Simulation statistical uncertainty
0.14	Jet energy scale
0.14	Renormalization and factorization scales
0.073	Modeling of b tagging
0.037	σ_{St} ($\sigma_t + \sigma_{\bar{t}}$)
0.035	Jet energy resolution
0.026	Modeling of pileup
0.023	$Wb\bar{b}$ content
0.021	Ratio of St cross sections, $\sigma_t/\sigma_{\bar{t}}$
0.021	Modeling of $t\bar{t}$ production
0.018	PDFs
<0.010	$\mathcal{L}$, σ_{DY}, δ_{Wj}, trigger ϵ_μ, F^e_{Mj}, $\delta_{t\bar{t}}$, α_s
<0.001	Trigger ϵ_e, p_T^t, ID_e, ID_μ, F^μ_{Mj}
0.33	Total

6 Results

The measured sample composition is presented in Table 3. Figure 10 shows the data from each

Table 3: Results from the fit of the sample composition, in thousands of events, for the e+jets and μ+jets channels. The statistical uncertainty in the last digit is indicated in parentheses. The results of the simultaneous fit in both channels are included only for comparison and are not used in the measurement of A_c^y.

	Thousands of events						
	$t\bar{t}$	Wj	Mj	St	DY	Total	Observed
e only	207.1(8)	49.1(9)	50(1)	14.0	5.4	326(2)	326.185
μ only	242.5(8)	58.9(6)	18.7(5)	16.5	4.3	341(1)	340.911
Simultaneous fit e	207.1(5)	49.5(4)	50.2(6)	14.0	5.4	326.2(9)	326.185
μ	242.6(6)	58.8(5)	18.7(5)	16.5	4.3	340.9(9)	340.911

channel projected along $Y^{rec}_{t\bar{t}}$ and Δ, overlaid with the results of the fitted model.

Curves of the negative logarithm of the likelihood for both channels are shown in Fig. 11, along with the combined 68% confidence interval for A_c^y. The predictions of POWHEG, Kühn and Rodrigo [8], and Bernreuther and Si [9] are also plotted. Subfigures of Fig. 11 show the range of the antisymmetric components covered by the models at ± 1 standard deviation of the statistical uncertainty. The combined charge asymmetry using both channels is $A_c^y = [0.33 \pm 0.26\,(\text{stat}) \pm 0.33\,(\text{syst})]\%$, which is tabulated with the predictions in Table 4. The combined uncertainty is 0.42%.

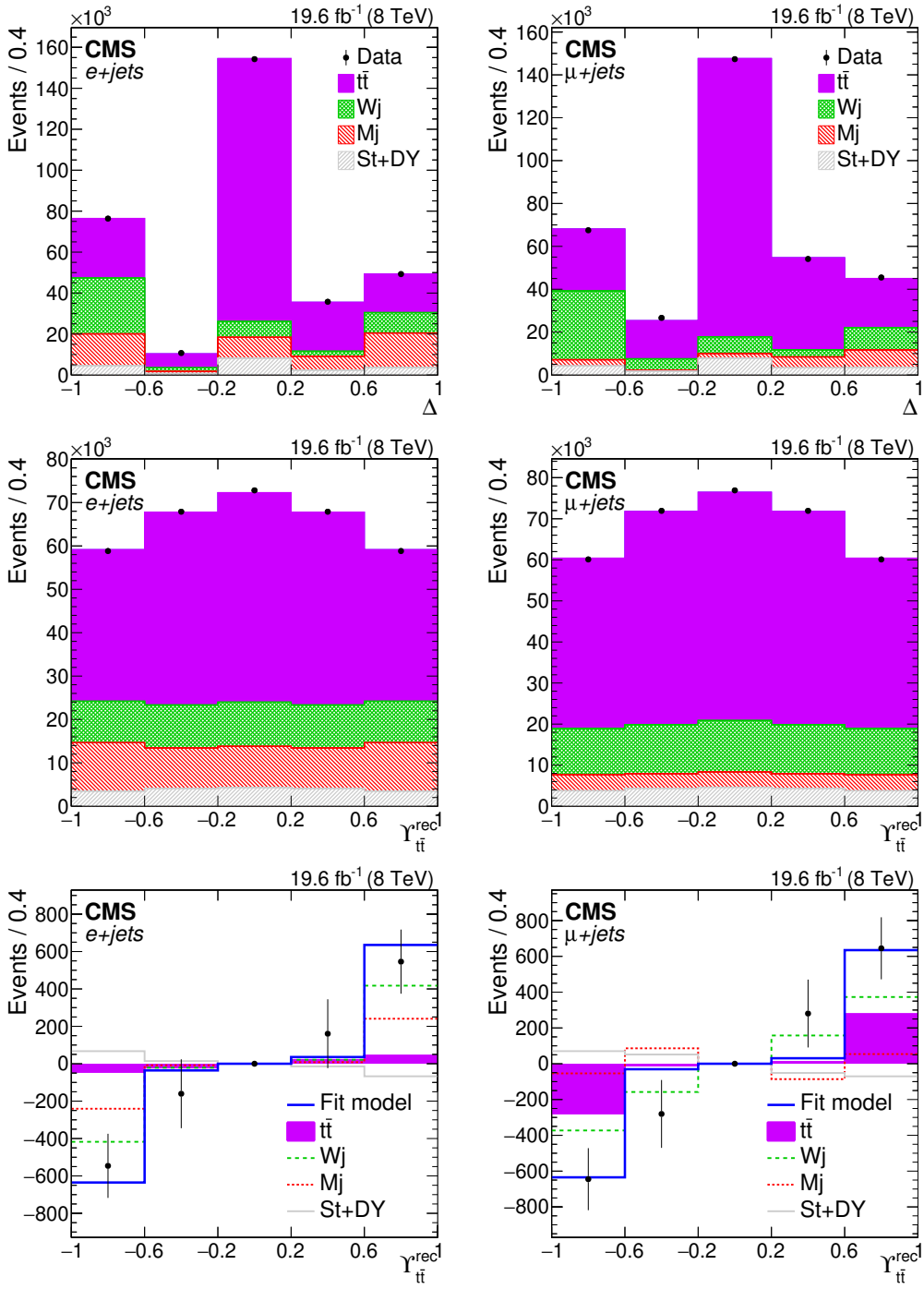

Figure 10: Sample composition is measured using the discriminant Δ distribution (top), in a model with contributions from $t\bar{t}$, Wj, Mj, and St + DY. With the sample composition subsequently fixed, the amplitude of the antisymmetric $t\bar{t}$ contribution is measured in the $\Upsilon^{\mathrm{rec}}_{t\bar{t}}$ distribution, shown decomposed into symmetric (middle) and antisymmetric (bottom) components. The thick line shows the antisymmetric component of the fit model. The measurements are performed independently on the (left) e+jets and (right) μ+jets samples.

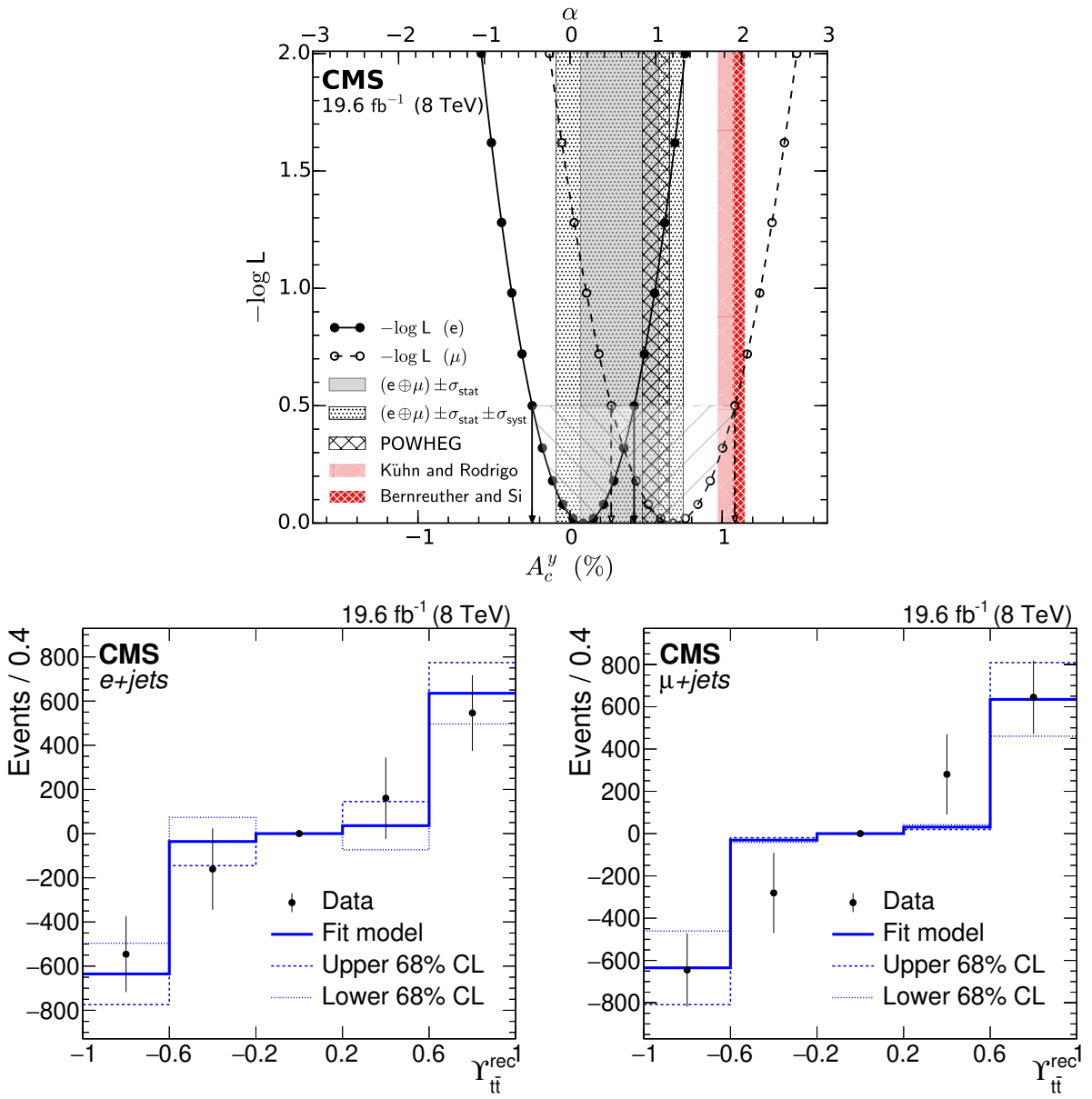

Figure 11: At top, the negative logarithm of the likelihood is shown as a function of α (upper axis) and A_c^y (lower axis), for e+jets (closed circles) and μ+jets (open circles) measurements. The statistical uncertainty in each is given by the intersections of the parabolas with $-\log L = 0.5$, which are marked by arrows. The 68% confidence interval of the combined A_c^y measurement is compared with those of the SM predictions by POWHEG, Kühn and Rodrigo [8], and Bernreuther and Si [9]. At bottom, the antisymmetric component of the $\Upsilon_{t\bar{t}}^{rec}$ distributions in data and the model are shown for (left) e+jets and (right) μ+jets, for the central value (solid), and for the upper (dashed) and lower (dotted) limits of the 68% statistical confidence intervals.

Table 4: Comparison of charge asymmetry measurements and predictions.

Source	$A_c^y(\%)$
e+jets	0.09 ± 0.34 (stat)
μ+jets	0.68 ± 0.41 (stat)
Combined	0.33 ± 0.26 (stat) $\pm$ 0.33 (syst)
POWHEG CT10	0.56 ± 0.09
MC@NLO	0.53 ± 0.09
Kühn and Rodrigo [8]	1.02 ± 0.05
Bernreuther and Si [9]	1.11 ± 0.04

The measured $\mathrm{t\bar{t}}$ production charge asymmetry A_c^y is compatible with another CMS $\sqrt{s} = 8$ TeV measurement [19], which uses an unfolding technique on the same data, and with the most recent Monte Carlo predictions and theoretical calculations. The template method incorporates more information from the model than used in comparable unfolding techniques [15–19] by using the distribution of the antisymmetric component of the probability density. This extra information carries the benefit of reduced statistical uncertainty, at the expense of greater model dependence, reflected in the systematic uncertainty. The contributions to the uncertainty from statistical and systematic sources are comparable in size. Since the systematic uncertainty is dominated by the statistical uncertainty in the templates, it can be reduced in future analyses through increased numbers of events in the simulation and in the sidebands in the data. The uncertainty in the POWHEG prediction arises from systematic uncertainties in the PDFs, the renormalization and factorization scales, and the strong coupling constant. A graphical comparison of the results and predictions is shown in Fig. 12.

7 Summary

The forward-central $\mathrm{t\bar{t}}$ charge asymmetry in proton-proton collisions at 8 TeV center-of-mass energy has been measured using lepton+jets events from data corresponding to an integrated luminosity of 19.6 fb^{-1}. Novel techniques in top quark reconstruction and background discrimination have been employed, which are likely to be of interest in future analyses. The measurement utilizes a template technique based on a parametrization of the SM. The result, $A_c^y = [0.33 \pm 0.26\,(\mathrm{stat}) \pm 0.33\,(\mathrm{syst})]\%$, is the most precise to date. It is consistent with SM predictions, but does not rule out the alternative models considered.

Acknowledgments

We congratulate our colleagues in the CERN accelerator departments for the excellent performance of the LHC and thank the technical and administrative staffs at CERN and at other CMS institutes for their contributions to the success of the CMS effort. In addition, we gratefully acknowledge the computing centers and personnel of the Worldwide LHC Computing Grid for delivering so effectively the computing infrastructure essential to our analyses. Finally, we acknowledge the enduring support for the construction and operation of the LHC and the CMS detector provided by the following funding agencies: the Austrian Federal Ministry of Science, Research and Economy and the Austrian Science Fund; the Belgian Fonds de la Recherche Scientifique, and Fonds voor Wetenschappelijk Onderzoek; the Brazilian Funding Agencies (CNPq, CAPES, FAPERJ, and FAPESP); the Bulgarian Ministry of Education and Science; CERN; the Chinese Academy of Sciences, Ministry of Science and Technology, and National Natural Science Foundation of China; the Colombian Funding Agency (COLCIENCIAS);

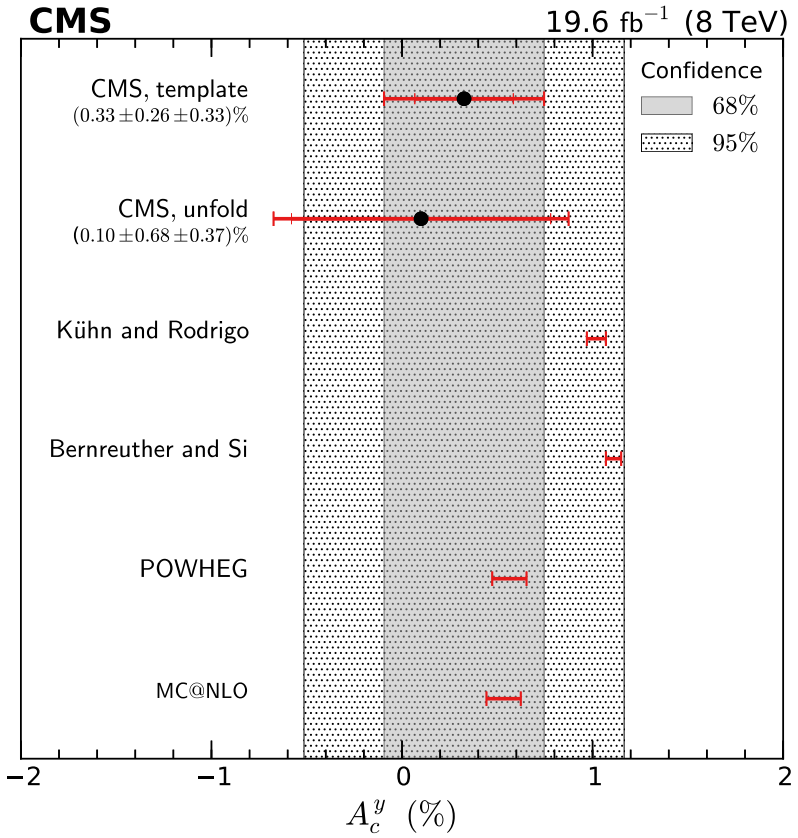

Figure 12: Comparison of results from this analysis (template) with those of the CMS 8 TeV unfolding analysis [19], and SM predictions from theoretical calculations of Kühn and Rodrigo [8], Bernreuther and Si [9], POWHEG, and MC@NLO. The shaded bands correspond to 68% and 95% confidence intervals of the current measurement. The inner bars on the CMS measurements indicate the statistical uncertainty, the outer bars the statistical and systematic uncertainty added in quadrature.

the Croatian Ministry of Science, Education and Sport, and the Croatian Science Foundation; the Research Promotion Foundation, Cyprus; the Ministry of Education and Research, Estonian Research Council via IUT23-4 and IUT23-6 and European Regional Development Fund, Estonia; the Academy of Finland, Finnish Ministry of Education and Culture, and Helsinki Institute of Physics; the Institut National de Physique Nucléaire et de Physique des Particules / CNRS, and Commissariat à l'Énergie Atomique et aux Énergies Alternatives / CEA, France; the Bundesministerium für Bildung und Forschung, Deutsche Forschungsgemeinschaft, and Helmholtz-Gemeinschaft Deutscher Forschungszentren, Germany; the General Secretariat for Research and Technology, Greece; the National Scientific Research Foundation, and National Innovation Office, Hungary; the Department of Atomic Energy and the Department of Science and Technology, India; the Institute for Studies in Theoretical Physics and Mathematics, Iran; the Science Foundation, Ireland; the Istituto Nazionale di Fisica Nucleare, Italy; the Ministry of Science, ICT and Future Planning, and National Research Foundation (NRF), Republic of Korea; the Lithuanian Academy of Sciences; the Ministry of Education, and University of Malaya (Malaysia); the Mexican Funding Agencies (CINVESTAV, CONACYT, SEP, and UASLP-FAI); the Ministry of Business, Innovation and Employment, New Zealand; the Pakistan Atomic Energy Commission; the Ministry of Science and Higher Education and the National Science Centre, Poland; the Fundação para a Ciência e a Tecnologia, Portugal; JINR, Dubna; the Ministry of Education and Science of the Russian Federation, the Federal Agency of

Atomic Energy of the Russian Federation, Russian Academy of Sciences, and the Russian Foundation for Basic Research; the Ministry of Education, Science and Technological Development of Serbia; the Secretaría de Estado de Investigación, Desarrollo e Innovación and Programa Consolider-Ingenio 2010, Spain; the Swiss Funding Agencies (ETH Board, ETH Zurich, PSI, SNF, UniZH, Canton Zurich, and SER); the Ministry of Science and Technology, Taipei; the Thailand Center of Excellence in Physics, the Institute for the Promotion of Teaching Science and Technology of Thailand, Special Task Force for Activating Research and the National Science and Technology Development Agency of Thailand; the Scientific and Technical Research Council of Turkey, and Turkish Atomic Energy Authority; the National Academy of Sciences of Ukraine, and State Fund for Fundamental Researches, Ukraine; the Science and Technology Facilities Council, UK; the US Department of Energy, and the US National Science Foundation.

Individuals have received support from the Marie-Curie program and the European Research Council and EPLANET (European Union); the Leventis Foundation; the A. P. Sloan Foundation; the Alexander von Humboldt Foundation; the Belgian Federal Science Policy Office; the Fonds pour la Formation à la Recherche dans l'Industrie et dans l'Agriculture (FRIA-Belgium); the Agentschap voor Innovatie door Wetenschap en Technologie (IWT-Belgium); the Ministry of Education, Youth and Sports (MEYS) of the Czech Republic; the Council of Science and Industrial Research, India; the HOMING PLUS program of the Foundation for Polish Science, cofinanced from European Union, Regional Development Fund; the OPUS program of the National Science Center (Poland); the Compagnia di San Paolo (Torino); the Consorzio per la Fisica (Trieste); MIUR project 20108T4XTM (Italy); the Thalis and Aristeia programs cofinanced by EU-ESF and the Greek NSRF; the National Priorities Research Program by Qatar National Research Fund; the Rachadapisek Sompot Fund for Postdoctoral Fellowship, Chulalongkorn University (Thailand); and the Welch Foundation, contract C-1845.

References

[1] Particle Data Group Collaboration, "Review of Particle Physics", *Chin. Phys. C* **38** (2014) 090001, doi:10.1088/1674-1137/38/9/090001.

[2] P. H. Frampton and S. L. Glashow, "Chiral Color: An Alternative to the Standard Model", *Phys. Lett. B* **190** (1987) 157, doi:10.1016/0370-2693(87)90859-8.

[3] R. Budny, "Effects of neutral weak currents in annihilation", *Phys. Lett. B* **45** (1973) 340, doi:10.1016/0370-2693(73)90050-6.

[4] D0 Collaboration, "Forward-backward asymmetry in top quark-antiquark production", *Phys. Rev. D* **84** (2011) 112005, doi:10.1103/PhysRevD.84.112005, arXiv:1107.4995.

[5] CDF Collaboration, "Evidence for a Mass Dependent Forward-Backward Asymmetry in Top Quark Pair Production", *Phys. Rev. D* **83** (2011) 112003, doi:10.1103/PhysRevD.83.112003, arXiv:1101.0034.

[6] CDF Collaboration, "Measurement of the top quark forward-backward production asymmetry and its dependence on event kinematic properties", *Phys. Rev. D* **87** (2013) 092002, doi:10.1103/PhysRevD.87.092002, arXiv:1211.1003.

[7] D0 Collaboration, "Measurement of the forward-backward asymmetry in top quark-antiquark production in $p\bar{p}$ collisions using the lepton + jets channel", *Phys. Rev. D* **90** (2014) 072011, doi:10.1103/PhysRevD.90.072011, arXiv:1405.0421.

[8] J. H. Kühn and G. Rodrigo, "Charge asymmetries of top quarks at hadron colliders revisited", *JHEP* **01** (2012) 063, doi:10.1007/JHEP01(2012)063, arXiv:1109.6830.

[9] W. Bernreuther and Z.-G. Si, "Top quark and leptonic charge asymmetries for the Tevatron and LHC", *Phys. Rev. D* **86** (2012) 034026, doi:10.1103/PhysRevD.86.034026, arXiv:1205.6580.

[10] CMS Collaboration, "Search for narrow resonances using the dijet mass spectrum in pp collisions at $\sqrt{s} = 8$ TeV", *Phys. Rev. D* **87** (2013) 114015, doi:10.1103/PhysRevD.87.114015, arXiv:1302.4794.

[11] ATLAS Collaboration, "Search for new phenomena in the dijet mass distribution using pp collision data at $\sqrt{s} = 8$ TeV with the ATLAS detector", *Phys. Rev. D* **91** (2015) 052007, doi:10.1103/PhysRevD.91.052007, arXiv:1407.1376.

[12] ATLAS Collaboration, "ATLAS search for new phenomena in dijet mass and angular distributions using pp collisions at $\sqrt{s} = 7$ TeV", *JHEP* **01** (2013) 029, doi:10.1007/JHEP01(2013)029, arXiv:1210.1718.

[13] A. Carmona et al., "From Tevatron's top and lepton-based asymmetries to the LHC", *JHEP* **07** (2014) 005, doi:10.1007/JHEP07(2014)005, arXiv:1401.2443.

[14] A. Atre, R. S. Chivukula, P. Ittisamai, and E. H. Simmons, "Distinguishing color-octet and color-singlet resonances at the Large Hadron Collider", *Phys. Rev. D* **88** (2013) 055021, doi:10.1103/PhysRevD.88.055021, arXiv:1306.4715.

[15] CMS Collaboration, "Measurement of the charge asymmetry in top-quark pair production in proton-proton collisions at $\sqrt{s} = 7$ TeV", *Phys. Lett. B* **709** (2012) 28, doi:10.1016/j.physletb.2012.01.078, arXiv:1112.5100.

[16] CMS Collaboration, "Inclusive and differential measurements of the $\mathrm{t\bar{t}}$ charge asymmetry in proton-proton collisions at $\sqrt{s} = 7$ TeV", *Phys. Lett. B* **717** (2012) 129, doi:10.1016/j.physletb.2012.09.028, arXiv:1207.0065.

[17] ATLAS Collaboration, "Measurement of the charge asymmetry in top quark pair production in pp collisions at $\sqrt{s} = 7$ TeV using the ATLAS detector", *Eur. Phys. J. C* **72** (2012) 2039, doi:10.1140/epjc/s10052-012-2039-5, arXiv:1203.4211.

[18] ATLAS Collaboration, "Measurement of the top quark pair production charge asymmetry in proton-proton collisions at $\sqrt{s} = 7$ TeV using the ATLAS detector", *JHEP* **02** (2014) 107, doi:10.1007/JHEP02(2014)107, arXiv:1311.6724.

[19] CMS Collaboration, "Inclusive and differential measurements of the $\mathrm{t\bar{t}}$ charge asymmetry in pp collisions at $\sqrt{s} = 8$ TeV", (2015). arXiv:1507.03119. Submitted to *Phys. Lett. B*.

[20] S. Frixione, P. Nason, and G. Ridolfi, "A positive-weight next-to-leading-order Monte Carlo for heavy flavour hadroproduction", *JHEP* **09** (2007) 126, doi:10.1088/1126-6708/2007/09/126, arXiv:0707.3088.

[21] H.-L. Lai et al., "New parton distributions for collider physics", *Phys. Rev. D* **82** (2010) 074024, doi:10.1103/PhysRevD.82.074024, arXiv:1007.2241.

[22] CMS Collaboration, "Particle–Flow Event Reconstruction in CMS and Performance for Jets, Taus, and $E_{\mathrm{T}}^{\mathrm{miss}}$", CMS Physics Analysis Summary CMS-PAS-PFT-09-001, 2009.

[23] CMS Collaboration, "Commissioning of the Particle-flow Event Reconstruction with the first LHC collisions recorded in the CMS detector", CMS Physics Analysis Summary CMS-PAS-PFT-10-001, 2010.

[24] CMS Collaboration, "Performance of electron reconstruction and selection with the CMS detector in proton-proton collisions at $\sqrt{s} = 8$ TeV", *JINST* **10** (2015) P06005, doi:10.1088/1748-0221/10/06/P06005, arXiv:1502.02701.

[25] M. Cacciari, G. P. Salam, and G. Soyez, "The anti-k_t jet clustering algorithm", *JHEP* **04** (2008) 063, doi:10.1088/1126-6708/2008/04/063, arXiv:0802.1189.

[26] CMS Collaboration, "Determination of jet energy calibration and transverse momentum resolution in CMS", *JINST* **6** (2011) P11002, doi:10.1088/1748-0221/6/11/P11002, arXiv:1107.4277.

[27] CMS Collaboration, "Identification of b-quark jets with the CMS experiment", *JINST* **8** (2013) P04013, doi:10.1088/1748-0221/8/04/P04013, arXiv:1211.4462.

[28] CMS Collaboration, "The CMS experiment at the CERN LHC", *JINST* **3** (2008) S08004, doi:10.1088/1748-0221/3/08/S08004.

[29] J. L. Leonard, "Luminosity measurement at CMS", in *Proceedings, 3rd International Conference on Technology and Instrumentation in Particle Physics (TIPP 2014)*, p. 348. SISSA, 2014. PoS(TIPP2014)348.

[30] CMS Collaboration, "Performance of CMS muon reconstruction in pp collision events at $\sqrt{s} = 7$ TeV", *JINST* **7** (2012) P10002, doi:10.1088/1748-0221/7/10/P10002, arXiv:1206.4071.

[31] GEANT4 Collaboration, "GEANT4—simulation toolkit", *Nucl. Instrum. Meth. A* **506** (2003) 250, doi:10.1016/S0168-9002(03)01368-8.

[32] T. Sjöstrand, S. Mrenna, and P. Z. Skands, "PYTHIA 6.4 physics and manual", *JHEP* **05** (2006) 026, doi:10.1088/1126-6708/2006/05/026, arXiv:hep-ph/0603175.

[33] T. Sjöstrand, S. Mrenna, and P. Z. Skands, "A Brief Introduction to PYTHIA 8.1", *Comput. Phys. Commun.* **178** (2008) 852, doi:10.1016/j.cpc.2008.01.036, arXiv:0710.3820.

[34] R. Corke and T. Sjöstrand, "Improved Parton Showers at Large Transverse Momenta", *Eur. Phys. J. C* **69** (2010) 1, doi:10.1140/epjc/s10052-010-1409-0, arXiv:1003.2384.

[35] J. Alwall et al., "MadGraph 5: going beyond", *JHEP* **06** (2011) 128, doi:10.1007/JHEP06(2011)128, arXiv:1106.0522.

[36] S. Alioli, P. Nason, C. Oleari, and E. Re, "NLO single-top production matched with shower in POWHEG: s- and t-channel contributions", *JHEP* **09** (2009) 111, doi:10.1088/1126-6708/2009/09/111, arXiv:0907.4076. [Erratum: doi:10.1007/JHEP02(2010)011].

[37] E. Re, "Single-top W t-channel production matched with parton showers using the POWHEG method", *Eur. Phys. J. C* **71** (2011) 1547, doi:10.1140/epjc/s10052-011-1547-z, arXiv:1009.2450.

[38] S. Frixione and B. R. Webber, "Matching NLO QCD computations and parton shower simulations", *JHEP* **06** (2002) 029, doi:10.1088/1126-6708/2002/06/029, arXiv:hep-ph/0204244.

[39] J. Pumplin et al., "Parton distributions and the strong coupling: CTEQ6AB PDFs", *JHEP* **02** (2006) 032, doi:10.1088/1126-6708/2006/02/032, arXiv:hep-ph/0512167.

[40] A. Giammanco, "The Fast Simulation of the CMS Experiment", *J. Phys. Conf. Ser.* **513** (2014) 022012, doi:10.1088/1742-6596/513/2/022012.

[41] S. Jung, A. Pierce, and J. D. Wells, "Top quark asymmetry from a non-Abelian horizontal symmetry", *Phys. Rev. D* **83** (2011) 114039, doi:10.1103/PhysRevD.83.114039, arXiv:1103.4835.

[42] B. A. Betchart, R. Demina, and A. Harel, "Analytic solutions for neutrino momenta in decay of top quarks", *Nucl. Instrum. Meth. A* **736** (2014) 169, doi:10.1016/j.nima.2013.10.039, arXiv:1305.1878.

[43] B. L. Welch, "Note on Discriminant Functions", *Biometrika* **31** (1939) 218, doi:10.2307/2334985.

[44] W. Verkerke and D. P. Kirkby, "The RooFit toolkit for data modeling", in *Proceedings of the 13th Int. Conf. for Computing in High-Energy and Nuclear Phys.* 2003. arXiv:physics/0306116.

[45] M. Botje et al., "The PDF4LHC Working Group Interim Recommendations", (2011). arXiv:1101.0538.

A The CMS Collaboration

Yerevan Physics Institute, Yerevan, Armenia
V. Khachatryan, A.M. Sirunyan, A. Tumasyan

Institut für Hochenergiephysik der OeAW, Wien, Austria
W. Adam, E. Asilar, T. Bergauer, J. Brandstetter, E. Brondolin, M. Dragicevic, J. Erö, M. Flechl, M. Friedl, R. Frühwirth[1], V.M. Ghete, C. Hartl, N. Hörmann, J. Hrubec, M. Jeitler[1], V. Knünz, A. König, M. Krammer[1], I. Krätschmer, D. Liko, T. Matsushita, I. Mikulec, D. Rabady[2], B. Rahbaran, H. Rohringer, J. Schieck[1], R. Schöfbeck, J. Strauss, W. Treberer-Treberspurg, W. Waltenberger, C.-E. Wulz[1]

National Centre for Particle and High Energy Physics, Minsk, Belarus
V. Mossolov, N. Shumeiko, J. Suarez Gonzalez

Universiteit Antwerpen, Antwerpen, Belgium
S. Alderweireldt, T. Cornelis, E.A. De Wolf, X. Janssen, A. Knutsson, J. Lauwers, S. Luyckx, S. Ochesanu, R. Rougny, M. Van De Klundert, H. Van Haevermaet, P. Van Mechelen, N. Van Remortel, A. Van Spilbeeck

Vrije Universiteit Brussel, Brussel, Belgium
S. Abu Zeid, F. Blekman, J. D'Hondt, N. Daci, I. De Bruyn, K. Deroover, N. Heracleous, J. Keaveney, S. Lowette, L. Moreels, A. Olbrechts, Q. Python, D. Strom, S. Tavernier, W. Van Doninck, P. Van Mulders, G.P. Van Onsem, I. Van Parijs

Université Libre de Bruxelles, Bruxelles, Belgium
P. Barria, C. Caillol, B. Clerbaux, G. De Lentdecker, H. Delannoy, G. Fasanella, L. Favart, A.P.R. Gay, A. Grebenyuk, T. Lenzi, A. Léonard, T. Maerschalk, A. Marinov, L. Perniè, A. Randle-conde, T. Reis, T. Seva, C. Vander Velde, P. Vanlaer, R. Yonamine, F. Zenoni, F. Zhang[3]

Ghent University, Ghent, Belgium
K. Beernaert, L. Benucci, A. Cimmino, S. Crucy, D. Dobur, A. Fagot, G. Garcia, M. Gul, J. Mccartin, A.A. Ocampo Rios, D. Poyraz, D. Ryckbosch, S. Salva, M. Sigamani, N. Strobbe, M. Tytgat, W. Van Driessche, E. Yazgan, N. Zaganidis

Université Catholique de Louvain, Louvain-la-Neuve, Belgium
S. Basegmez, C. Beluffi[4], O. Bondu, S. Brochet, G. Bruno, R. Castello, A. Caudron, L. Ceard, G.G. Da Silveira, C. Delaere, D. Favart, L. Forthomme, A. Giammanco[5], J. Hollar, A. Jafari, P. Jez, M. Komm, V. Lemaitre, A. Mertens, C. Nuttens, L. Perrini, A. Pin, K. Piotrzkowski, A. Popov[6], L. Quertenmont, M. Selvaggi, M. Vidal Marono

Université de Mons, Mons, Belgium
N. Beliy, G.H. Hammad

Centro Brasileiro de Pesquisas Fisicas, Rio de Janeiro, Brazil
W.L. Aldá Júnior, G.A. Alves, L. Brito, M. Correa Martins Junior, M. Hamer, C. Hensel, C. Mora Herrera, A. Moraes, M.E. Pol, P. Rebello Teles

Universidade do Estado do Rio de Janeiro, Rio de Janeiro, Brazil
E. Belchior Batista Das Chagas, W. Carvalho, J. Chinellato[7], A. Custódio, E.M. Da Costa, D. De Jesus Damiao, C. De Oliveira Martins, S. Fonseca De Souza, L.M. Huertas Guativa, H. Malbouisson, D. Matos Figueiredo, L. Mundim, H. Nogima, W.L. Prado Da Silva, A. Santoro, A. Sznajder, E.J. Tonelli Manganote[7], A. Vilela Pereira

Universidade Estadual Paulista [a], Universidade Federal do ABC [b], São Paulo, Brazil
S. Ahuja[a], C.A. Bernardes[b], A. De Souza Santos[b], S. Dogra[a], T.R. Fernandez Perez Tomei[a], E.M. Gregores[b], P.G. Mercadante[b], C.S. Moon[a,8], S.F. Novaes[a], Sandra S. Padula[a], D. Romero Abad, J.C. Ruiz Vargas

Institute for Nuclear Research and Nuclear Energy, Sofia, Bulgaria
A. Aleksandrov, V. Genchev†, R. Hadjiiska, P. Iaydjiev, S. Piperov, M. Rodozov, S. Stoykova, G. Sultanov, M. Vutova

University of Sofia, Sofia, Bulgaria
A. Dimitrov, I. Glushkov, L. Litov, B. Pavlov, P. Petkov

Institute of High Energy Physics, Beijing, China
M. Ahmad, J.G. Bian, G.M. Chen, H.S. Chen, M. Chen, T. Cheng, R. Du, C.H. Jiang, R. Plestina[9], F. Romeo, S.M. Shaheen, J. Tao, C. Wang, Z. Wang, H. Zhang

State Key Laboratory of Nuclear Physics and Technology, Peking University, Beijing, China
C. Asawatangtrakuldee, Y. Ban, Q. Li, S. Liu, Y. Mao, S.J. Qian, D. Wang, Z. Xu, W. Zou

Universidad de Los Andes, Bogota, Colombia
C. Avila, A. Cabrera, L.F. Chaparro Sierra, C. Florez, J.P. Gomez, B. Gomez Moreno, J.C. Sanabria

University of Split, Faculty of Electrical Engineering, Mechanical Engineering and Naval Architecture, Split, Croatia
N. Godinovic, D. Lelas, D. Polic, I. Puljak, P.M. Ribeiro Cipriano

University of Split, Faculty of Science, Split, Croatia
Z. Antunovic, M. Kovac

Institute Rudjer Boskovic, Zagreb, Croatia
V. Brigljevic, K. Kadija, J. Luetic, S. Micanovic, L. Sudic

University of Cyprus, Nicosia, Cyprus
A. Attikis, G. Mavromanolakis, J. Mousa, C. Nicolaou, F. Ptochos, P.A. Razis, H. Rykaczewski

Charles University, Prague, Czech Republic
M. Bodlak, M. Finger[10], M. Finger Jr.[10]

Academy of Scientific Research and Technology of the Arab Republic of Egypt, Egyptian Network of High Energy Physics, Cairo, Egypt
A.A. Abdelalim[11], T. Elkafrawy[12], A. Mahrous[13], A. Radi[14,12]

National Institute of Chemical Physics and Biophysics, Tallinn, Estonia
B. Calpas, M. Kadastik, M. Murumaa, M. Raidal, A. Tiko, C. Veelken

Department of Physics, University of Helsinki, Helsinki, Finland
P. Eerola, J. Pekkanen, M. Voutilainen

Helsinki Institute of Physics, Helsinki, Finland
J. Härkönen, V. Karimäki, R. Kinnunen, T. Lampén, K. Lassila-Perini, S. Lehti, T. Lindén, P. Luukka, T. Mäenpää, T. Peltola, E. Tuominen, J. Tuominiemi, E. Tuovinen, L. Wendland

Lappeenranta University of Technology, Lappeenranta, Finland
J. Talvitie, T. Tuuva

DSM/IRFU, CEA/Saclay, Gif-sur-Yvette, France
M. Besancon, F. Couderc, M. Dejardin, D. Denegri, B. Fabbro, J.L. Faure, C. Favaro, F. Ferri, S. Ganjour, A. Givernaud, P. Gras, G. Hamel de Monchenault, P. Jarry, E. Locci, M. Machet, J. Malcles, J. Rander, A. Rosowsky, M. Titov, A. Zghiche

Laboratoire Leprince-Ringuet, Ecole Polytechnique, IN2P3-CNRS, Palaiseau, France
I. Antropov, S. Baffioni, F. Beaudette, P. Busson, L. Cadamuro, E. Chapon, C. Charlot, T. Dahms, O. Davignon, N. Filipovic, A. Florent, R. Granier de Cassagnac, S. Lisniak, L. Mastrolorenzo, P. Miné, I.N. Naranjo, M. Nguyen, C. Ochando, G. Ortona, P. Paganini, S. Regnard, R. Salerno, J.B. Sauvan, Y. Sirois, T. Strebler, Y. Yilmaz, A. Zabi

Institut Pluridisciplinaire Hubert Curien, Université de Strasbourg, Université de Haute Alsace Mulhouse, CNRS/IN2P3, Strasbourg, France
J.-L. Agram[15], J. Andrea, A. Aubin, D. Bloch, J.-M. Brom, M. Buttignol, E.C. Chabert, N. Chanon, C. Collard, E. Conte[15], X. Coubez, J.-C. Fontaine[15], D. Gelé, U. Goerlach, C. Goetzmann, A.-C. Le Bihan, J.A. Merlin[2], K. Skovpen, P. Van Hove

Centre de Calcul de l'Institut National de Physique Nucleaire et de Physique des Particules, CNRS/IN2P3, Villeurbanne, France
S. Gadrat

Université de Lyon, Université Claude Bernard Lyon 1, CNRS-IN2P3, Institut de Physique Nucléaire de Lyon, Villeurbanne, France
S. Beauceron, C. Bernet, G. Boudoul, E. Bouvier, C.A. Carrillo Montoya, J. Chasserat, R. Chierici, D. Contardo, B. Courbon, P. Depasse, H. El Mamouni, J. Fan, J. Fay, S. Gascon, M. Gouzevitch, B. Ille, F. Lagarde, I.B. Laktineh, M. Lethuillier, L. Mirabito, A.L. Pequegnot, S. Perries, J.D. Ruiz Alvarez, D. Sabes, L. Sgandurra, V. Sordini, M. Vander Donckt, P. Verdier, S. Viret, H. Xiao

Georgian Technical University, Tbilisi, Georgia
T. Toriashvili[16]

Tbilisi State University, Tbilisi, Georgia
Z. Tsamalaidze[10]

RWTH Aachen University, I. Physikalisches Institut, Aachen, Germany
C. Autermann, S. Beranek, M. Edelhoff, L. Feld, A. Heister, M.K. Kiesel, K. Klein, M. Lipinski, A. Ostapchuk, M. Preuten, F. Raupach, S. Schael, J.F. Schulte, T. Verlage, H. Weber, B. Wittmer, V. Zhukov[6]

RWTH Aachen University, III. Physikalisches Institut A, Aachen, Germany
M. Ata, M. Brodski, E. Dietz-Laursonn, D. Duchardt, M. Endres, M. Erdmann, S. Erdweg, T. Esch, R. Fischer, A. Güth, T. Hebbeker, C. Heidemann, K. Hoepfner, D. Klingebiel, S. Knutzen, P. Kreuzer, M. Merschmeyer, A. Meyer, P. Millet, M. Olschewski, K. Padeken, P. Papacz, T. Pook, M. Radziej, H. Reithler, M. Rieger, F. Scheuch, L. Sonnenschein, D. Teyssier, S. Thüer

RWTH Aachen University, III. Physikalisches Institut B, Aachen, Germany
V. Cherepanov, Y. Erdogan, G. Flügge, H. Geenen, M. Geisler, F. Hoehle, B. Kargoll, T. Kress, Y. Kuessel, A. Künsken, J. Lingemann[2], A. Nehrkorn, A. Nowack, I.M. Nugent, C. Pistone, O. Pooth, A. Stahl

Deutsches Elektronen-Synchrotron, Hamburg, Germany
M. Aldaya Martin, I. Asin, N. Bartosik, O. Behnke, U. Behrens, A.J. Bell, K. Borras, A. Burgmeier, A. Cakir, L. Calligaris, A. Campbell, S. Choudhury, F. Costanza, C. Diez

Pardos, G. Dolinska, S. Dooling, T. Dorland, G. Eckerlin, D. Eckstein, T. Eichhorn, G. Flucke, E. Gallo, J. Garay Garcia, A. Geiser, A. Gizhko, P. Gunnellini, J. Hauk, M. Hempel[17], H. Jung, A. Kalogeropoulos, O. Karacheban[17], M. Kasemann, P. Katsas, J. Kieseler, C. Kleinwort, I. Korol, W. Lange, J. Leonard, K. Lipka, A. Lobanov, W. Lohmann[17], R. Mankel, I. Marfin[17], I.-A. Melzer-Pellmann, A.B. Meyer, G. Mittag, J. Mnich, A. Mussgiller, S. Naumann-Emme, A. Nayak, E. Ntomari, H. Perrey, D. Pitzl, R. Placakyte, A. Raspereza, B. Roland, M.Ö. Sahin, P. Saxena, T. Schoerner-Sadenius, M. Schröder, C. Seitz, S. Spannagel, K.D. Trippkewitz, R. Walsh, C. Wissing

University of Hamburg, Hamburg, Germany
V. Blobel, M. Centis Vignali, A.R. Draeger, J. Erfle, E. Garutti, K. Goebel, D. Gonzalez, M. Görner, J. Haller, M. Hoffmann, R.S. Höing, A. Junkes, R. Klanner, R. Kogler, T. Lapsien, T. Lenz, I. Marchesini, D. Marconi, D. Nowatschin, J. Ott, F. Pantaleo[2], T. Peiffer, A. Perieanu, N. Pietsch, J. Poehlsen, D. Rathjens, C. Sander, H. Schettler, P. Schleper, E. Schlieckau, A. Schmidt, J. Schwandt, M. Seidel, V. Sola, H. Stadie, G. Steinbrück, H. Tholen, D. Troendle, E. Usai, L. Vanelderen, A. Vanhoefer

Institut für Experimentelle Kernphysik, Karlsruhe, Germany
M. Akbiyik, C. Barth, C. Baus, J. Berger, C. Böser, E. Butz, T. Chwalek, F. Colombo, W. De Boer, A. Descroix, A. Dierlamm, S. Fink, F. Frensch, M. Giffels, A. Gilbert, F. Hartmann[2], S.M. Heindl, U. Husemann, I. Katkov[6], A. Kornmayer[2], P. Lobelle Pardo, B. Maier, H. Mildner, M.U. Mozer, T. Müller, Th. Müller, M. Plagge, G. Quast, K. Rabbertz, S. Röcker, F. Roscher, H.J. Simonis, F.M. Stober, R. Ulrich, J. Wagner-Kuhr, S. Wayand, M. Weber, T. Weiler, C. Wöhrmann, R. Wolf

Institute of Nuclear and Particle Physics (INPP), NCSR Demokritos, Aghia Paraskevi, Greece
G. Anagnostou, G. Daskalakis, T. Geralis, V.A. Giakoumopoulou, A. Kyriakis, D. Loukas, A. Psallidas, I. Topsis-Giotis

University of Athens, Athens, Greece
A. Agapitos, S. Kesisoglou, A. Panagiotou, N. Saoulidou, E. Tziaferi

University of Ioánnina, Ioánnina, Greece
I. Evangelou, G. Flouris, C. Foudas, P. Kokkas, N. Loukas, N. Manthos, I. Papadopoulos, E. Paradas, J. Strologas

Wigner Research Centre for Physics, Budapest, Hungary
G. Bencze, C. Hajdu, A. Hazi, P. Hidas, D. Horvath[18], F. Sikler, V. Veszpremi, G. Vesztergombi[19], A.J. Zsigmond

Institute of Nuclear Research ATOMKI, Debrecen, Hungary
N. Beni, S. Czellar, J. Karancsi[20], J. Molnar, Z. Szillasi

University of Debrecen, Debrecen, Hungary
M. Bartók[21], A. Makovec, P. Raics, Z.L. Trocsanyi, B. Ujvari

National Institute of Science Education and Research, Bhubaneswar, India
P. Mal, K. Mandal, N. Sahoo, S.K. Swain

Panjab University, Chandigarh, India
S. Bansal, S.B. Beri, V. Bhatnagar, R. Chawla, R. Gupta, U.Bhawandeep, A.K. Kalsi, A. Kaur, M. Kaur, R. Kumar, A. Mehta, M. Mittal, J.B. Singh, G. Walia

University of Delhi, Delhi, India
Ashok Kumar, Arun Kumar, A. Bhardwaj, B.C. Choudhary, R.B. Garg, A. Kumar, S. Malhotra, M. Naimuddin, N. Nishu, K. Ranjan, R. Sharma, V. Sharma

Saha Institute of Nuclear Physics, Kolkata, India
S. Banerjee, S. Bhattacharya, K. Chatterjee, S. Dey, S. Dutta, Sa. Jain, N. Majumdar, A. Modak, K. Mondal, S. Mukherjee, S. Mukhopadhyay, A. Roy, D. Roy, S. Roy Chowdhury, S. Sarkar, M. Sharan

Bhabha Atomic Research Centre, Mumbai, India
A. Abdulsalam, R. Chudasama, D. Dutta, V. Jha, V. Kumar, A.K. Mohanty[2], L.M. Pant, P. Shukla, A. Topkar

Tata Institute of Fundamental Research, Mumbai, India
T. Aziz, S. Banerjee, S. Bhowmik[22], R.M. Chatterjee, R.K. Dewanjee, S. Dugad, S. Ganguly, S. Ghosh, M. Guchait, A. Gurtu[23], G. Kole, S. Kumar, B. Mahakud, M. Maity[22], G. Majumder, K. Mazumdar, S. Mitra, G.B. Mohanty, B. Parida, T. Sarkar[22], K. Sudhakar, N. Sur, B. Sutar, N. Wickramage[24]

Indian Institute of Science Education and Research (IISER), Pune, India
S. Chauhan, S. Dube, S. Sharma

Institute for Research in Fundamental Sciences (IPM), Tehran, Iran
H. Bakhshiansohi, H. Behnamian, S.M. Etesami[25], A. Fahim[26], R. Goldouzian, M. Khakzad, M. Mohammadi Najafabadi, M. Naseri, S. Paktinat Mehdiabadi, F. Rezaei Hosseinabadi, B. Safarzadeh[27], M. Zeinali

University College Dublin, Dublin, Ireland
M. Felcini, M. Grunewald

INFN Sezione di Bari [a], Università di Bari [b], Politecnico di Bari [c], Bari, Italy
M. Abbrescia[a,b], C. Calabria[a,b], C. Caputo[a,b], S.S. Chhibra[a,b], A. Colaleo[a], D. Creanza[a,c], L. Cristella[a,b], N. De Filippis[a,c], M. De Palma[a,b], L. Fiore[a], G. Iaselli[a,c], G. Maggi[a,c], M. Maggi[a], G. Miniello[a,b], S. My[a,c], S. Nuzzo[a,b], A. Pompili[a,b], G. Pugliese[a,c], R. Radogna[a,b], A. Ranieri[a], G. Selvaggi[a,b], L. Silvestris[a,2], R. Venditti[a,b], P. Verwilligen[a]

INFN Sezione di Bologna [a], Università di Bologna [b], Bologna, Italy
G. Abbiendi[a], C. Battilana[2], A.C. Benvenuti[a], D. Bonacorsi[a,b], S. Braibant-Giacomelli[a,b], L. Brigliadori[a,b], R. Campanini[a,b], P. Capiluppi[a,b], A. Castro[a,b], F.R. Cavallo[a], G. Codispoti[a,b], M. Cuffiani[a,b], G.M. Dallavalle[a], F. Fabbri[a], A. Fanfani[a,b], D. Fasanella[a,b], P. Giacomelli[a], C. Grandi[a], L. Guiducci[a,b], S. Marcellini[a], G. Masetti[a], A. Montanari[a], F.L. Navarria[a,b], A. Perrotta[a], A.M. Rossi[a,b], T. Rovelli[a,b], G.P. Siroli[a,b], N. Tosi[a,b], R. Travaglini[a,b]

INFN Sezione di Catania [a], Università di Catania [b], CSFNSM [c], Catania, Italy
G. Cappello[a], M. Chiorboli[a,b], S. Costa[a,b], F. Giordano[a], R. Potenza[a,b], A. Tricomi[a,b], C. Tuve[a,b]

INFN Sezione di Firenze [a], Università di Firenze [b], Firenze, Italy
G. Barbagli[a], V. Ciulli[a,b], C. Civinini[a], R. D'Alessandro[a,b], E. Focardi[a,b], S. Gonzi[a,b], V. Gori[a,b], P. Lenzi[a,b], M. Meschini[a], S. Paoletti[a], G. Sguazzoni[a], A. Tropiano[a,b], L. Viliani[a,b]

INFN Laboratori Nazionali di Frascati, Frascati, Italy
L. Benussi, S. Bianco, F. Fabbri, D. Piccolo

INFN Sezione di Genova [a], Università di Genova [b], Genova, Italy
V. Calvelli[a,b], F. Ferro[a], M. Lo Vetere[a,b], M.R. Monge[a,b], E. Robutti[a], S. Tosi[a,b]

INFN Sezione di Milano-Bicocca [a], Università di Milano-Bicocca [b], Milano, Italy
L. Brianza, M.E. Dinardo[a,b], S. Fiorendi[a,b], S. Gennai[a], R. Gerosa[a,b], A. Ghezzi[a,b], P. Govoni[a,b], S. Malvezzi[a], R.A. Manzoni[a,b], B. Marzocchi[a,b,2], D. Menasce[a], L. Moroni[a], M. Paganoni[a,b], D. Pedrini[a], S. Ragazzi[a,b], N. Redaelli[a], T. Tabarelli de Fatis[a,b]

INFN Sezione di Napoli [a], Università di Napoli 'Federico II' [b], Napoli, Italy, Università della Basilicata [c], Potenza, Italy, Università G. Marconi [d], Roma, Italy
S. Buontempo[a], N. Cavallo[a,c], S. Di Guida[a,d,2], M. Esposito[a,b], F. Fabozzi[a,c], A.O.M. Iorio[a,b], G. Lanza[a], L. Lista[a], S. Meola[a,d,2], M. Merola[a], P. Paolucci[a,2], C. Sciacca[a,b], F. Thyssen

INFN Sezione di Padova [a], Università di Padova [b], Padova, Italy, Università di Trento [c], Trento, Italy
P. Azzi[a,2], N. Bacchetta[a], L. Benato[a,b], D. Bisello[a,b], A. Boletti[a,b], A. Branca[a,b], R. Carlin[a,b], P. Checchia[a], M. Dall'Osso[a,b,2], T. Dorigo[a], F. Fanzago[a], F. Gasparini[a,b], U. Gasparini[a,b], A. Gozzelino[a], K. Kanishchev[a,c], S. Lacaprara[a], M. Margoni[a,b], A.T. Meneguzzo[a,b], J. Pazzini[a,b], N. Pozzobon[a,b], P. Ronchese[a,b], F. Simonetto[a,b], E. Torassa[a], M. Tosi[a,b], S. Ventura[a], M. Zanetti, P. Zotto[a,b], A. Zucchetta[a,b,2], G. Zumerle[a,b]

INFN Sezione di Pavia [a], Università di Pavia [b], Pavia, Italy
A. Braghieri[a], A. Magnani[a], P. Montagna[a,b], S.P. Ratti[a,b], V. Re[a], C. Riccardi[a,b], P. Salvini[a], I. Vai[a], P. Vitulo[a,b]

INFN Sezione di Perugia [a], Università di Perugia [b], Perugia, Italy
L. Alunni Solestizi[a,b], M. Biasini[a,b], G.M. Bilei[a], D. Ciangottini[a,b,2], L. Fanò[a,b], P. Lariccia[a,b], G. Mantovani[a,b], M. Menichelli[a], A. Saha[a], A. Santocchia[a,b], A. Spiezia[a,b]

INFN Sezione di Pisa [a], Università di Pisa [b], Scuola Normale Superiore di Pisa [c], Pisa, Italy
K. Androsov[a,28], P. Azzurri[a], G. Bagliesi[a], J. Bernardini[a], T. Boccali[a], G. Broccolo[a,c], R. Castaldi[a], M.A. Ciocci[a,28], R. Dell'Orso[a], S. Donato[a,c,2], G. Fedi, L. Foà[a,c†], A. Giassi[a], M.T. Grippo[a,28], F. Ligabue[a,c], T. Lomtadze[a], L. Martini[a,b], A. Messineo[a,b], F. Palla[a], A. Rizzi[a,b], A. Savoy-Navarro[a,29], A.T. Serban[a], P. Spagnolo[a], P. Squillacioti[a,28], R. Tenchini[a], G. Tonelli[a,b], A. Venturi[a], P.G. Verdini[a]

INFN Sezione di Roma [a], Università di Roma [b], Roma, Italy
L. Barone[a,b], F. Cavallari[a], G. D'imperio[a,b,2], D. Del Re[a,b], M. Diemoz[a], S. Gelli[a,b], C. Jorda[a], E. Longo[a,b], F. Margaroli[a,b], P. Meridiani[a], F. Micheli[a,b], G. Organtini[a,b], R. Paramatti[a], F. Preiato[a,b], S. Rahatlou[a,b], C. Rovelli[a], F. Santanastasio[a,b], P. Traczyk[a,b,2]

INFN Sezione di Torino [a], Università di Torino [b], Torino, Italy, Università del Piemonte Orientale [c], Novara, Italy
N. Amapane[a,b], R. Arcidiacono[a,c,2], S. Argiro[a,b], M. Arneodo[a,c], R. Bellan[a,b], C. Biino[a], N. Cartiglia[a], M. Costa[a,b], R. Covarelli[a,b], P. De Remigis[a], A. Degano[a,b], N. Demaria[a], L. Finco[a,b,2], C. Mariotti[a], S. Maselli[a], E. Migliore[a,b], V. Monaco[a,b], E. Monteil[a,b], M. Musich[a], M.M. Obertino[a,b], L. Pacher[a,b], N. Pastrone[a], M. Pelliccioni[a], G.L. Pinna Angioni[a,b], F. Ravera[a,b], A. Romero[a,b], M. Ruspa[a,c], R. Sacchi[a,b], A. Solano[a,b], A. Staiano[a], U. Tamponi[a]

INFN Sezione di Trieste [a], Università di Trieste [b], Trieste, Italy
S. Belforte[a], V. Candelise[a,b,2], M. Casarsa[a], F. Cossutti[a], G. Della Ricca[a,b], B. Gobbo[a], C. La Licata[a,b], M. Marone[a,b], A. Schizzi[a,b], T. Umer[a,b], A. Zanetti[a]

Kangwon National University, Chunchon, Korea
S. Chang, A. Kropivnitskaya, S.K. Nam

Kyungpook National University, Daegu, Korea
D.H. Kim, G.N. Kim, M.S. Kim, D.J. Kong, S. Lee, Y.D. Oh, A. Sakharov, D.C. Son

Chonbuk National University, Jeonju, Korea
J.A. Brochero Cifuentes, H. Kim, T.J. Kim, M.S. Ryu

Chonnam National University, Institute for Universe and Elementary Particles, Kwangju, Korea
S. Song

Korea University, Seoul, Korea
S. Choi, Y. Go, D. Gyun, B. Hong, M. Jo, H. Kim, Y. Kim, B. Lee, K. Lee, K.S. Lee, S. Lee, S.K. Park, Y. Roh

Seoul National University, Seoul, Korea
H.D. Yoo

University of Seoul, Seoul, Korea
M. Choi, H. Kim, J.H. Kim, J.S.H. Lee, I.C. Park, G. Ryu

Sungkyunkwan University, Suwon, Korea
Y. Choi, Y.K. Choi, J. Goh, D. Kim, E. Kwon, J. Lee, I. Yu

Vilnius University, Vilnius, Lithuania
A. Juodagalvis, J. Vaitkus

National Centre for Particle Physics, Universiti Malaya, Kuala Lumpur, Malaysia
I. Ahmed, Z.A. Ibrahim, J.R. Komaragiri, M.A.B. Md Ali[30], F. Mohamad Idris[31], W.A.T. Wan Abdullah, M.N. Yusli

Centro de Investigacion y de Estudios Avanzados del IPN, Mexico City, Mexico
E. Casimiro Linares, H. Castilla-Valdez, E. De La Cruz-Burelo, I. Heredia-de La Cruz[32], A. Hernandez-Almada, R. Lopez-Fernandez, A. Sanchez-Hernandez

Universidad Iberoamericana, Mexico City, Mexico
S. Carrillo Moreno, F. Vazquez Valencia

Benemerita Universidad Autonoma de Puebla, Puebla, Mexico
S. Carpinteyro, I. Pedraza, H.A. Salazar Ibarguen

Universidad Autónoma de San Luis Potosí, San Luis Potosí, Mexico
A. Morelos Pineda

University of Auckland, Auckland, New Zealand
D. Krofcheck

University of Canterbury, Christchurch, New Zealand
P.H. Butler, S. Reucroft

National Centre for Physics, Quaid-I-Azam University, Islamabad, Pakistan
A. Ahmad, M. Ahmad, Q. Hassan, H.R. Hoorani, W.A. Khan, T. Khurshid, M. Shoaib

National Centre for Nuclear Research, Swierk, Poland
H. Bialkowska, M. Bluj, B. Boimska, T. Frueboes, M. Górski, M. Kazana, K. Nawrocki, K. Romanowska-Rybinska, M. Szleper, P. Zalewski

Institute of Experimental Physics, Faculty of Physics, University of Warsaw, Warsaw, Poland
G. Brona, K. Bunkowski, K. Doroba, A. Kalinowski, M. Konecki, J. Krolikowski, M. Misiura, M. Olszewski, M. Walczak

Laboratório de Instrumentação e Física Experimental de Partículas, Lisboa, Portugal
P. Bargassa, C. Beirão Da Cruz E Silva, A. Di Francesco, P. Faccioli, P.G. Ferreira Parracho, M. Gallinaro, N. Leonardo, L. Lloret Iglesias, F. Nguyen, J. Rodrigues Antunes, J. Seixas, O. Toldaiev, D. Vadruccio, J. Varela, P. Vischia

Joint Institute for Nuclear Research, Dubna, Russia
S. Afanasiev, P. Bunin, M. Gavrilenko, I. Golutvin, I. Gorbunov, A. Kamenev, V. Karjavin, V. Konoplyanikov, A. Lanev, A. Malakhov, V. Matveev[33], P. Moisenz, V. Palichik, V. Perelygin, S. Shmatov, S. Shulha, N. Skatchkov, V. Smirnov, A. Zarubin

Petersburg Nuclear Physics Institute, Gatchina (St. Petersburg), Russia
V. Golovtsov, Y. Ivanov, V. Kim[34], E. Kuznetsova, P. Levchenko, V. Murzin, V. Oreshkin, I. Smirnov, V. Sulimov, L. Uvarov, S. Vavilov, A. Vorobyev

Institute for Nuclear Research, Moscow, Russia
Yu. Andreev, A. Dermenev, S. Gninenko, N. Golubev, A. Karneyeu, M. Kirsanov, N. Krasnikov, A. Pashenkov, D. Tlisov, A. Toropin

Institute for Theoretical and Experimental Physics, Moscow, Russia
V. Epshteyn, V. Gavrilov, N. Lychkovskaya, V. Popov, I. Pozdnyakov, G. Safronov, A. Spiridonov, E. Vlasov, A. Zhokin

National Research Nuclear University 'Moscow Engineering Physics Institute' (MEPhI), Moscow, Russia
A. Bylinkin

P.N. Lebedev Physical Institute, Moscow, Russia
V. Andreev, M. Azarkin[35], I. Dremin[35], M. Kirakosyan, A. Leonidov[35], G. Mesyats, S.V. Rusakov, A. Vinogradov

Skobeltsyn Institute of Nuclear Physics, Lomonosov Moscow State University, Moscow, Russia
A. Baskakov, A. Belyaev, E. Boos, V. Bunichev, M. Dubinin[36], L. Dudko, A. Gribushin, V. Klyukhin, N. Korneeva, I. Lokhtin, I. Myagkov, S. Obraztsov, M. Perfilov, V. Savrin, A. Snigirev

State Research Center of Russian Federation, Institute for High Energy Physics, Protvino, Russia
I. Azhgirey, I. Bayshev, S. Bitioukov, V. Kachanov, A. Kalinin, D. Konstantinov, V. Krychkine, V. Petrov, R. Ryutin, A. Sobol, L. Tourtchanovitch, S. Troshin, N. Tyurin, A. Uzunian, A. Volkov

University of Belgrade, Faculty of Physics and Vinca Institute of Nuclear Sciences, Belgrade, Serbia
P. Adzic[37], M. Ekmedzic, J. Milosevic, V. Rekovic

Centro de Investigaciones Energéticas Medioambientales y Tecnológicas (CIEMAT), Madrid, Spain
J. Alcaraz Maestre, E. Calvo, M. Cerrada, M. Chamizo Llatas, N. Colino, B. De La Cruz, A. Delgado Peris, D. Domínguez Vázquez, A. Escalante Del Valle, C. Fernandez Bedoya, J.P. Fernández Ramos, J. Flix, M.C. Fouz, P. Garcia-Abia, O. Gonzalez Lopez, S. Goy Lopez,

J.M. Hernandez, M.I. Josa, E. Navarro De Martino, A. Pérez-Calero Yzquierdo, J. Puerta Pelayo, A. Quintario Olmeda, I. Redondo, L. Romero, M.S. Soares

Universidad Autónoma de Madrid, Madrid, Spain
C. Albajar, J.F. de Trocóniz, M. Missiroli, D. Moran

Universidad de Oviedo, Oviedo, Spain
H. Brun, J. Cuevas, J. Fernandez Menendez, S. Folgueras, I. Gonzalez Caballero, E. Palencia Cortezon, J.M. Vizan Garcia

Instituto de Física de Cantabria (IFCA), CSIC-Universidad de Cantabria, Santander, Spain
I.J. Cabrillo, A. Calderon, J.R. Castiñeiras De Saa, P. De Castro Manzano, J. Duarte Campderros, M. Fernandez, G. Gomez, A. Graziano, A. Lopez Virto, J. Marco, R. Marco, C. Martinez Rivero, F. Matorras, F.J. Munoz Sanchez, J. Piedra Gomez, T. Rodrigo, A.Y. Rodríguez-Marrero, A. Ruiz-Jimeno, L. Scodellaro, I. Vila, R. Vilar Cortabitarte

CERN, European Organization for Nuclear Research, Geneva, Switzerland
D. Abbaneo, E. Auffray, G. Auzinger, M. Bachtis, P. Baillon, A.H. Ball, D. Barney, A. Benaglia, J. Bendavid, L. Benhabib, J.F. Benitez, G.M. Berruti, P. Bloch, A. Bocci, A. Bonato, C. Botta, H. Breuker, T. Camporesi, G. Cerminara, S. Colafranceschi[38], M. D'Alfonso, D. d'Enterria, A. Dabrowski, V. Daponte, A. David, M. De Gruttola, F. De Guio, A. De Roeck, S. De Visscher, E. Di Marco, M. Dobson, M. Dordevic, B. Dorney, T. du Pree, N. Dupont, A. Elliott-Peisert, G. Franzoni, W. Funk, D. Gigi, K. Gill, D. Giordano, M. Girone, F. Glege, R. Guida, S. Gundacker, M. Guthoff, J. Hammer, P. Harris, J. Hegeman, V. Innocente, P. Janot, H. Kirschenmann, M.J. Kortelainen, K. Kousouris, K. Krajczar, P. Lecoq, C. Lourenço, M.T. Lucchini, N. Magini, L. Malgeri, M. Mannelli, A. Martelli, L. Masetti, F. Meijers, S. Mersi, E. Meschi, F. Moortgat, S. Morovic, M. Mulders, M.V. Nemallapudi, H. Neugebauer, S. Orfanelli[39], L. Orsini, L. Pape, E. Perez, A. Petrilli, G. Petrucciani, A. Pfeiffer, D. Piparo, A. Racz, G. Rolandi[40], M. Rovere, M. Ruan, H. Sakulin, C. Schäfer, C. Schwick, A. Sharma, P. Silva, M. Simon, P. Sphicas[41], D. Spiga, J. Steggemann, B. Stieger, M. Stoye, Y. Takahashi, D. Treille, A. Triossi, A. Tsirou, G.I. Veres[19], N. Wardle, H.K. Wöhri, A. Zagozdzinska[42], W.D. Zeuner

Paul Scherrer Institut, Villigen, Switzerland
W. Bertl, K. Deiters, W. Erdmann, R. Horisberger, Q. Ingram, H.C. Kaestli, D. Kotlinski, U. Langenegger, D. Renker, T. Rohe

Institute for Particle Physics, ETH Zurich, Zurich, Switzerland
F. Bachmair, L. Bäni, L. Bianchini, M.A. Buchmann, B. Casal, G. Dissertori, M. Dittmar, M. Donegà, M. Dünser, P. Eller, C. Grab, C. Heidegger, D. Hits, J. Hoss, G. Kasieczka, W. Lustermann, B. Mangano, A.C. Marini, M. Marionneau, P. Martinez Ruiz del Arbol, M. Masciovecchio, D. Meister, P. Musella, F. Nessi-Tedaldi, F. Pandolfi, J. Pata, F. Pauss, L. Perrozzi, M. Peruzzi, M. Quittnat, M. Rossini, A. Starodumov[43], M. Takahashi, V.R. Tavolaro, K. Theofilatos, R. Wallny

Universität Zürich, Zurich, Switzerland
T.K. Aarrestad, C. Amsler[44], L. Caminada, M.F. Canelli, V. Chiochia, A. De Cosa, C. Galloni, A. Hinzmann, T. Hreus, B. Kilminster, C. Lange, J. Ngadiuba, D. Pinna, P. Robmann, F.J. Ronga, D. Salerno, Y. Yang

National Central University, Chung-Li, Taiwan
M. Cardaci, K.H. Chen, T.H. Doan, C. Ferro, Sh. Jain, R. Khurana, M. Konyushikhin, C.M. Kuo, W. Lin, Y.J. Lu, R. Volpe, S.S. Yu

National Taiwan University (NTU), Taipei, Taiwan
R. Bartek, P. Chang, Y.H. Chang, Y.W. Chang, Y. Chao, K.F. Chen, P.H. Chen, C. Dietz, F. Fiori, U. Grundler, W.-S. Hou, Y. Hsiung, Y.F. Liu, R.-S. Lu, M. Miñano Moya, E. Petrakou, J.F. Tsai, Y.M. Tzeng

Chulalongkorn University, Faculty of Science, Department of Physics, Bangkok, Thailand
B. Asavapibhop, K. Kovitanggoon, G. Singh, N. Srimanobhas, N. Suwonjandee

Cukurova University, Adana, Turkey
A. Adiguzel, S. Cerci[45], C. Dozen, S. Girgis, G. Gokbulut, Y. Guler, E. Gurpinar, I. Hos, E.E. Kangal[46], A. Kayis Topaksu, G. Onengut[47], K. Ozdemir[48], S. Ozturk[49], B. Tali[45], H. Topakli[49], M. Vergili, C. Zorbilmez

Middle East Technical University, Physics Department, Ankara, Turkey
I.V. Akin, B. Bilin, S. Bilmis, B. Isildak[50], G. Karapinar[51], U.E. Surat, M. Yalvac, M. Zeyrek

Bogazici University, Istanbul, Turkey
E.A. Albayrak[52], E. Gülmez, M. Kaya[53], O. Kaya[54], T. Yetkin[55]

Istanbul Technical University, Istanbul, Turkey
K. Cankocak, S. Sen[56], F.I. Vardarlı

Institute for Scintillation Materials of National Academy of Science of Ukraine, Kharkov, Ukraine
B. Grynyov

National Scientific Center, Kharkov Institute of Physics and Technology, Kharkov, Ukraine
L. Levchuk, P. Sorokin

University of Bristol, Bristol, United Kingdom
R. Aggleton, F. Ball, L. Beck, J.J. Brooke, E. Clement, D. Cussans, H. Flacher, J. Goldstein, M. Grimes, G.P. Heath, H.F. Heath, J. Jacob, L. Kreczko, C. Lucas, Z. Meng, D.M. Newbold[57], S. Paramesvaran, A. Poll, T. Sakuma, S. Seif El Nasr-storey, S. Senkin, D. Smith, V.J. Smith

Rutherford Appleton Laboratory, Didcot, United Kingdom
K.W. Bell, A. Belyaev[58], C. Brew, R.M. Brown, D.J.A. Cockerill, J.A. Coughlan, K. Harder, S. Harper, E. Olaiya, D. Petyt, C.H. Shepherd-Themistocleous, A. Thea, L. Thomas, I.R. Tomalin, T. Williams, W.J. Womersley, S.D. Worm

Imperial College, London, United Kingdom
M. Baber, R. Bainbridge, O. Buchmuller, A. Bundock, D. Burton, S. Casasso, M. Citron, D. Colling, L. Corpe, N. Cripps, P. Dauncey, G. Davies, A. De Wit, M. Della Negra, P. Dunne, A. Elwood, W. Ferguson, J. Fulcher, D. Futyan, G. Hall, G. Iles, G. Karapostoli, M. Kenzie, R. Lane, R. Lucas[57], L. Lyons, A.-M. Magnan, S. Malik, J. Nash, A. Nikitenko[43], J. Pela, M. Pesaresi, K. Petridis, D.M. Raymond, A. Richards, A. Rose, C. Seez, A. Tapper, K. Uchida, M. Vazquez Acosta[59], T. Virdee, S.C. Zenz

Brunel University, Uxbridge, United Kingdom
J.E. Cole, P.R. Hobson, A. Khan, P. Kyberd, D. Leggat, D. Leslie, I.D. Reid, P. Symonds, L. Teodorescu, M. Turner

Baylor University, Waco, USA
A. Borzou, K. Call, J. Dittmann, K. Hatakeyama, A. Kasmi, H. Liu, N. Pastika

The University of Alabama, Tuscaloosa, USA
O. Charaf, S.I. Cooper, C. Henderson, P. Rumerio

Boston University, Boston, USA
A. Avetisyan, T. Bose, C. Fantasia, D. Gastler, P. Lawson, D. Rankin, C. Richardson, J. Rohlf, J. St. John, L. Sulak, D. Zou

Brown University, Providence, USA
J. Alimena, E. Berry, S. Bhattacharya, D. Cutts, N. Dhingra, A. Ferapontov, A. Garabedian, U. Heintz, E. Laird, G. Landsberg, Z. Mao, M. Narain, S. Sagir, T. Sinthuprasith

University of California, Davis, Davis, USA
R. Breedon, G. Breto, M. Calderon De La Barca Sanchez, S. Chauhan, M. Chertok, J. Conway, R. Conway, P.T. Cox, R. Erbacher, M. Gardner, W. Ko, R. Lander, M. Mulhearn, D. Pellett, J. Pilot, F. Ricci-Tam, S. Shalhout, J. Smith, M. Squires, D. Stolp, M. Tripathi, S. Wilbur, R. Yohay

University of California, Los Angeles, USA
R. Cousins, P. Everaerts, C. Farrell, J. Hauser, M. Ignatenko, D. Saltzberg, E. Takasugi, V. Valuev, M. Weber

University of California, Riverside, Riverside, USA
K. Burt, R. Clare, J. Ellison, J.W. Gary, G. Hanson, J. Heilman, M. Ivova PANEVA, P. Jandir, E. Kennedy, F. Lacroix, O.R. Long, A. Luthra, M. Malberti, M. Olmedo Negrete, A. Shrinivas, H. Wei, S. Wimpenny

University of California, San Diego, La Jolla, USA
J.G. Branson, G.B. Cerati, S. Cittolin, R.T. D'Agnolo, A. Holzner, R. Kelley, D. Klein, J. Letts, I. Macneill, D. Olivito, S. Padhi, M. Pieri, M. Sani, V. Sharma, S. Simon, M. Tadel, A. Vartak, S. Wasserbaech[60], C. Welke, F. Würthwein, A. Yagil, G. Zevi Della Porta

University of California, Santa Barbara, Santa Barbara, USA
D. Barge, J. Bradmiller-Feld, C. Campagnari, A. Dishaw, V. Dutta, K. Flowers, M. Franco Sevilla, P. Geffert, C. George, F. Golf, L. Gouskos, J. Gran, J. Incandela, C. Justus, N. Mccoll, S.D. Mullin, J. Richman, D. Stuart, I. Suarez, W. To, C. West, J. Yoo

California Institute of Technology, Pasadena, USA
D. Anderson, A. Apresyan, A. Bornheim, J. Bunn, Y. Chen, J. Duarte, A. Mott, H.B. Newman, C. Pena, M. Pierini, M. Spiropulu, J.R. Vlimant, S. Xie, R.Y. Zhu

Carnegie Mellon University, Pittsburgh, USA
V. Azzolini, A. Calamba, B. Carlson, T. Ferguson, Y. Iiyama, M. Paulini, J. Russ, M. Sun, H. Vogel, I. Vorobiev

University of Colorado Boulder, Boulder, USA
J.P. Cumalat, W.T. Ford, A. Gaz, F. Jensen, A. Johnson, M. Krohn, T. Mulholland, U. Nauenberg, J.G. Smith, K. Stenson, S.R. Wagner

Cornell University, Ithaca, USA
J. Alexander, A. Chatterjee, J. Chaves, J. Chu, S. Dittmer, N. Eggert, N. Mirman, G. Nicolas Kaufman, J.R. Patterson, A. Rinkevicius, A. Ryd, L. Skinnari, L. Soffi, W. Sun, S.M. Tan, W.D. Teo, J. Thom, J. Thompson, J. Tucker, Y. Weng, P. Wittich

Fermi National Accelerator Laboratory, Batavia, USA
S. Abdullin, M. Albrow, J. Anderson, G. Apollinari, L.A.T. Bauerdick, A. Beretvas, J. Berryhill, P.C. Bhat, G. Bolla, K. Burkett, J.N. Butler, H.W.K. Cheung, F. Chlebana, S. Cihangir, V.D. Elvira, I. Fisk, J. Freeman, E. Gottschalk, L. Gray, D. Green, S. Grünendahl, O. Gutsche, J. Hanlon, D. Hare, R.M. Harris, J. Hirschauer, B. Hooberman, Z. Hu, S. Jindariani, M. Johnson, U. Joshi, A.W. Jung, B. Klima, B. Kreis, S. Kwan[†], S. Lammel, J. Linacre, D. Lincoln, R. Lipton,

T. Liu, R. Lopes De Sá, J. Lykken, K. Maeshima, J.M. Marraffino, V.I. Martinez Outschoorn, S. Maruyama, D. Mason, P. McBride, P. Merkel, K. Mishra, S. Mrenna, S. Nahn, C. Newman-Holmes, V. O'Dell, K. Pedro, O. Prokofyev, G. Rakness, E. Sexton-Kennedy, A. Soha, W.J. Spalding, L. Spiegel, L. Taylor, S. Tkaczyk, N.V. Tran, L. Uplegger, E.W. Vaandering, C. Vernieri, M. Verzocchi, R. Vidal, H.A. Weber, A. Whitbeck, F. Yang, H. Yin

University of Florida, Gainesville, USA
D. Acosta, P. Avery, P. Bortignon, D. Bourilkov, A. Carnes, M. Carver, D. Curry, S. Das, G.P. Di Giovanni, R.D. Field, M. Fisher, I.K. Furic, J. Hugon, J. Konigsberg, A. Korytov, J.F. Low, P. Ma, K. Matchev, H. Mei, P. Milenovic[61], G. Mitselmakher, L. Muniz, D. Rank, R. Rossin, L. Shchutska, M. Snowball, D. Sperka, J. Wang, S. Wang, J. Yelton

Florida International University, Miami, USA
S. Hewamanage, S. Linn, P. Markowitz, G. Martinez, J.L. Rodriguez

Florida State University, Tallahassee, USA
A. Ackert, J.R. Adams, T. Adams, A. Askew, J. Bochenek, B. Diamond, J. Haas, S. Hagopian, V. Hagopian, K.F. Johnson, A. Khatiwada, H. Prosper, V. Veeraraghavan, M. Weinberg

Florida Institute of Technology, Melbourne, USA
M.M. Baarmand, V. Bhopatkar, M. Hohlmann, H. Kalakhety, D. Mareskas-palcek, T. Roy, F. Yumiceva

University of Illinois at Chicago (UIC), Chicago, USA
M.R. Adams, L. Apanasevich, D. Berry, R.R. Betts, I. Bucinskaite, R. Cavanaugh, O. Evdokimov, L. Gauthier, C.E. Gerber, D.J. Hofman, P. Kurt, C. O'Brien, I.D. Sandoval Gonzalez, C. Silkworth, P. Turner, N. Varelas, Z. Wu, M. Zakaria

The University of Iowa, Iowa City, USA
B. Bilki[62], W. Clarida, K. Dilsiz, S. Durgut, R.P. Gandrajula, M. Haytmyradov, V. Khristenko, J.-P. Merlo, H. Mermerkaya[63], A. Mestvirishvili, A. Moeller, J. Nachtman, H. Ogul, Y. Onel, F. Ozok[52], A. Penzo, C. Snyder, P. Tan, E. Tiras, J. Wetzel, K. Yi

Johns Hopkins University, Baltimore, USA
I. Anderson, B.A. Barnett, B. Blumenfeld, D. Fehling, L. Feng, A.V. Gritsan, P. Maksimovic, C. Martin, M. Osherson, M. Swartz, M. Xiao, Y. Xin, C. You

The University of Kansas, Lawrence, USA
P. Baringer, A. Bean, G. Benelli, C. Bruner, J. Gray, R.P. Kenny III, D. Majumder, M. Malek, M. Murray, D. Noonan, S. Sanders, R. Stringer, Q. Wang, J.S. Wood

Kansas State University, Manhattan, USA
I. Chakaberia, A. Ivanov, K. Kaadze, S. Khalil, M. Makouski, Y. Maravin, A. Mohammadi, L.K. Saini, N. Skhirtladze, I. Svintradze, S. Toda

Lawrence Livermore National Laboratory, Livermore, USA
D. Lange, F. Rebassoo, D. Wright

University of Maryland, College Park, USA
C. Anelli, A. Baden, O. Baron, A. Belloni, B. Calvert, S.C. Eno, C. Ferraioli, J.A. Gomez, N.J. Hadley, S. Jabeen, R.G. Kellogg, T. Kolberg, J. Kunkle, Y. Lu, A.C. Mignerey, Y.H. Shin, A. Skuja, M.B. Tonjes, S.C. Tonwar

Massachusetts Institute of Technology, Cambridge, USA
A. Apyan, R. Barbieri, A. Baty, K. Bierwagen, S. Brandt, W. Busza, I.A. Cali, Z. Demiragli, L. Di

Matteo, G. Gomez Ceballos, M. Goncharov, D. Gulhan, G.M. Innocenti, M. Klute, D. Kovalskyi, Y.S. Lai, Y.-J. Lee, A. Levin, P.D. Luckey, C. Mcginn, C. Mironov, X. Niu, C. Paus, D. Ralph, C. Roland, G. Roland, J. Salfeld-Nebgen, G.S.F. Stephans, K. Sumorok, M. Varma, D. Velicanu, J. Veverka, J. Wang, T.W. Wang, B. Wyslouch, M. Yang, V. Zhukova

University of Minnesota, Minneapolis, USA
B. Dahmes, A. Finkel, A. Gude, P. Hansen, S. Kalafut, S.C. Kao, K. Klapoetke, Y. Kubota, Z. Lesko, J. Mans, S. Nourbakhsh, N. Ruckstuhl, R. Rusack, N. Tambe, J. Turkewitz

University of Mississippi, Oxford, USA
J.G. Acosta, S. Oliveros

University of Nebraska-Lincoln, Lincoln, USA
E. Avdeeva, K. Bloom, S. Bose, D.R. Claes, A. Dominguez, C. Fangmeier, R. Gonzalez Suarez, R. Kamalieddin, J. Keller, D. Knowlton, I. Kravchenko, J. Lazo-Flores, F. Meier, J. Monroy, F. Ratnikov, J.E. Siado, G.R. Snow

State University of New York at Buffalo, Buffalo, USA
M. Alyari, J. Dolen, J. George, A. Godshalk, I. Iashvili, J. Kaisen, A. Kharchilava, A. Kumar, S. Rappoccio

Northeastern University, Boston, USA
G. Alverson, E. Barberis, D. Baumgartel, M. Chasco, A. Hortiangtham, A. Massironi, D.M. Morse, D. Nash, T. Orimoto, R. Teixeira De Lima, D. Trocino, R.-J. Wang, D. Wood, J. Zhang

Northwestern University, Evanston, USA
K.A. Hahn, A. Kubik, N. Mucia, N. Odell, B. Pollack, A. Pozdnyakov, M. Schmitt, S. Stoynev, K. Sung, M. Trovato, M. Velasco, S. Won

University of Notre Dame, Notre Dame, USA
A. Brinkerhoff, N. Dev, M. Hildreth, C. Jessop, D.J. Karmgard, N. Kellams, K. Lannon, S. Lynch, N. Marinelli, F. Meng, C. Mueller, Y. Musienko[33], T. Pearson, M. Planer, A. Reinsvold, R. Ruchti, G. Smith, S. Taroni, N. Valls, M. Wayne, M. Wolf, A. Woodard

The Ohio State University, Columbus, USA
L. Antonelli, J. Brinson, B. Bylsma, L.S. Durkin, S. Flowers, A. Hart, C. Hill, R. Hughes, K. Kotov, T.Y. Ling, B. Liu, W. Luo, D. Puigh, M. Rodenburg, B.L. Winer, H.W. Wulsin

Princeton University, Princeton, USA
O. Driga, P. Elmer, J. Hardenbrook, P. Hebda, S.A. Koay, P. Lujan, D. Marlow, T. Medvedeva, M. Mooney, J. Olsen, C. Palmer, P. Piroué, X. Quan, H. Saka, D. Stickland, C. Tully, J.S. Werner, A. Zuranski

University of Puerto Rico, Mayaguez, USA
S. Malik

Purdue University, West Lafayette, USA
V.E. Barnes, D. Benedetti, D. Bortoletto, L. Gutay, M.K. Jha, M. Jones, K. Jung, M. Kress, D.H. Miller, N. Neumeister, F. Primavera, B.C. Radburn-Smith, X. Shi, I. Shipsey, D. Silvers, J. Sun, A. Svyatkovskiy, F. Wang, W. Xie, L. Xu, J. Zablocki

Purdue University Calumet, Hammond, USA
N. Parashar, J. Stupak

Rice University, Houston, USA
A. Adair, B. Akgun, Z. Chen, K.M. Ecklund, F.J.M. Geurts, M. Guilbaud, W. Li, B. Michlin, M. Northup, B.P. Padley, R. Redjimi, J. Roberts, J. Rorie, Z. Tu, J. Zabel

University of Rochester, Rochester, USA
B. Betchart, A. Bodek, P. de Barbaro, R. Demina, Y. Eshaq, T. Ferbel, M. Galanti, A. Garcia-Bellido, P. Goldenzweig, J. Han, A. Harel, O. Hindrichs, A. Khukhunaishvili, G. Petrillo, M. Verzetti

The Rockefeller University, New York, USA
L. Demortier

Rutgers, The State University of New Jersey, Piscataway, USA
S. Arora, A. Barker, J.P. Chou, C. Contreras-Campana, E. Contreras-Campana, D. Duggan, D. Ferencek, Y. Gershtein, R. Gray, E. Halkiadakis, D. Hidas, E. Hughes, S. Kaplan, R. Kunnawalkam Elayavalli, A. Lath, K. Nash, S. Panwalkar, M. Park, S. Salur, S. Schnetzer, D. Sheffield, S. Somalwar, R. Stone, S. Thomas, P. Thomassen, M. Walker

University of Tennessee, Knoxville, USA
M. Foerster, G. Riley, K. Rose, S. Spanier, A. York

Texas A&M University, College Station, USA
O. Bouhali[64], A. Castaneda Hernandez, M. Dalchenko, M. De Mattia, A. Delgado, S. Dildick, R. Eusebi, W. Flanagan, J. Gilmore, T. Kamon[65], V. Krutelyov, R. Montalvo, R. Mueller, I. Osipenkov, Y. Pakhotin, R. Patel, A. Perloff, J. Roe, A. Rose, A. Safonov, A. Tatarinov, K.A. Ulmer[2]

Texas Tech University, Lubbock, USA
N. Akchurin, C. Cowden, J. Damgov, C. Dragoiu, P.R. Dudero, J. Faulkner, S. Kunori, K. Lamichhane, S.W. Lee, T. Libeiro, S. Undleeb, I. Volobouev

Vanderbilt University, Nashville, USA
E. Appelt, A.G. Delannoy, S. Greene, A. Gurrola, R. Janjam, W. Johns, C. Maguire, Y. Mao, A. Melo, P. Sheldon, B. Snook, S. Tuo, J. Velkovska, Q. Xu

University of Virginia, Charlottesville, USA
M.W. Arenton, S. Boutle, B. Cox, B. Francis, J. Goodell, R. Hirosky, A. Ledovskoy, H. Li, C. Lin, C. Neu, E. Wolfe, J. Wood, F. Xia

Wayne State University, Detroit, USA
C. Clarke, R. Harr, P.E. Karchin, C. Kottachchi Kankanamge Don, P. Lamichhane, J. Sturdy

University of Wisconsin, Madison, USA
D.A. Belknap, D. Carlsmith, M. Cepeda, A. Christian, S. Dasu, L. Dodd, S. Duric, E. Friis, B. Gomber, R. Hall-Wilton, M. Herndon, A. Hervé, P. Klabbers, A. Lanaro, A. Levine, K. Long, R. Loveless, A. Mohapatra, I. Ojalvo, T. Perry, G.A. Pierro, G. Polese, I. Ross, T. Ruggles, T. Sarangi, A. Savin, A. Sharma, N. Smith, W.H. Smith, D. Taylor, N. Woods

†: Deceased
1: Also at Vienna University of Technology, Vienna, Austria
2: Also at CERN, European Organization for Nuclear Research, Geneva, Switzerland
3: Also at State Key Laboratory of Nuclear Physics and Technology, Peking University, Beijing, China
4: Also at Institut Pluridisciplinaire Hubert Curien, Université de Strasbourg, Université de Haute Alsace Mulhouse, CNRS/IN2P3, Strasbourg, France

5: Also at National Institute of Chemical Physics and Biophysics, Tallinn, Estonia
6: Also at Skobeltsyn Institute of Nuclear Physics, Lomonosov Moscow State University, Moscow, Russia
7: Also at Universidade Estadual de Campinas, Campinas, Brazil
8: Also at Centre National de la Recherche Scientifique (CNRS) - IN2P3, Paris, France
9: Also at Laboratoire Leprince-Ringuet, Ecole Polytechnique, IN2P3-CNRS, Palaiseau, France
10: Also at Joint Institute for Nuclear Research, Dubna, Russia
11: Also at Zewail City of Science and Technology, Zewail, Egypt
12: Also at Ain Shams University, Cairo, Egypt
13: Also at Helwan University, Cairo, Egypt
14: Also at British University in Egypt, Cairo, Egypt
15: Also at Université de Haute Alsace, Mulhouse, France
16: Also at Tbilisi State University, Tbilisi, Georgia
17: Also at Brandenburg University of Technology, Cottbus, Germany
18: Also at Institute of Nuclear Research ATOMKI, Debrecen, Hungary
19: Also at Eötvös Loránd University, Budapest, Hungary
20: Also at University of Debrecen, Debrecen, Hungary
21: Also at Wigner Research Centre for Physics, Budapest, Hungary
22: Also at University of Visva-Bharati, Santiniketan, India
23: Now at King Abdulaziz University, Jeddah, Saudi Arabia
24: Also at University of Ruhuna, Matara, Sri Lanka
25: Also at Isfahan University of Technology, Isfahan, Iran
26: Also at University of Tehran, Department of Engineering Science, Tehran, Iran
27: Also at Plasma Physics Research Center, Science and Research Branch, Islamic Azad University, Tehran, Iran
28: Also at Università degli Studi di Siena, Siena, Italy
29: Also at Purdue University, West Lafayette, USA
30: Also at International Islamic University of Malaysia, Kuala Lumpur, Malaysia
31: Also at Malaysian Nuclear Agency, MOSTI, Kajang, Malaysia
32: Also at Consejo Nacional de Ciencia y Tecnología, Mexico city, Mexico
33: Also at Institute for Nuclear Research, Moscow, Russia
34: Also at St. Petersburg State Polytechnical University, St. Petersburg, Russia
35: Also at National Research Nuclear University 'Moscow Engineering Physics Institute' (MEPhI), Moscow, Russia
36: Also at California Institute of Technology, Pasadena, USA
37: Also at Faculty of Physics, University of Belgrade, Belgrade, Serbia
38: Also at Facoltà Ingegneria, Università di Roma, Roma, Italy
39: Also at National Technical University of Athens, Athens, Greece
40: Also at Scuola Normale e Sezione dell'INFN, Pisa, Italy
41: Also at University of Athens, Athens, Greece
42: Also at Warsaw University of Technology, Institute of Electronic Systems, Warsaw, Poland
43: Also at Institute for Theoretical and Experimental Physics, Moscow, Russia
44: Also at Albert Einstein Center for Fundamental Physics, Bern, Switzerland
45: Also at Adiyaman University, Adiyaman, Turkey
46: Also at Mersin University, Mersin, Turkey
47: Also at Cag University, Mersin, Turkey
48: Also at Piri Reis University, Istanbul, Turkey
49: Also at Gaziosmanpasa University, Tokat, Turkey
50: Also at Ozyegin University, Istanbul, Turkey

51: Also at Izmir Institute of Technology, Izmir, Turkey
52: Also at Mimar Sinan University, Istanbul, Istanbul, Turkey
53: Also at Marmara University, Istanbul, Turkey
54: Also at Kafkas University, Kars, Turkey
55: Also at Yildiz Technical University, Istanbul, Turkey
56: Also at Hacettepe University, Ankara, Turkey
57: Also at Rutherford Appleton Laboratory, Didcot, United Kingdom
58: Also at School of Physics and Astronomy, University of Southampton, Southampton, United Kingdom
59: Also at Instituto de Astrofísica de Canarias, La Laguna, Spain
60: Also at Utah Valley University, Orem, USA
61: Also at University of Belgrade, Faculty of Physics and Vinca Institute of Nuclear Sciences, Belgrade, Serbia
62: Also at Argonne National Laboratory, Argonne, USA
63: Also at Erzincan University, Erzincan, Turkey
64: Also at Texas A&M University at Qatar, Doha, Qatar
65: Also at Kyungpook National University, Daegu, Korea